POLITECNICO DI MILANO

Scuola di Ingegneria Industriale e dell'Informazione

Corso di Laurea Magistrale in Ingegneria Biomedica

Fabrication of Anatomical Models for Experimentation:

from CT Scans to 3D Silicone Models

Supervisor: Prof. Ing. Maria Laura Costantino

Co-supervisor: Francesco De Gaetano, PhD

Master thesis of:

Julie El Jurdi 885009

Academic Year 2020-2021

Table of Contents

List of Tables

List of Figures

Abstract

Introduction

Despite standard surgical techniques used to prevent any residual air in the chest after surgical interventions, significant amounts of air remain present and lead to embolization. To solve this problem, carbon dioxide field flooding has been proven to be an efficient technique in deairing the operative field and significantly reducing the risk of embolisms. This is due to the fact that carbon dioxide is denser than air and can take its place by gravity, and more importantly, due to its higher solubility in blood. With the rise of minimally invasive surgeries, the need for locally targeting microscopic areas with carbon dioxide instead of flooding the whole surgical field has risen. Studies are being done on optimizing catheters that allow the flow of carbon dioxide into the chest, targeting only the areas undergoing any exposure to the operatory field. To optimize these catheters, many factors must be designed such as the number of openings, the dimensions, the flowrate passing through them, the type of flow, and more. The most ideal method to determine these parameters is through experimentation.

The objective of this study is to help create a setup identical to that of the surgical field in order to carry out experiments that allow us to optimize the parameters of carbon dioxide catheters. The most important element of the setup, which will be discussed in detail, is the model of the organ which will be targeted by the catheter. This study provides a step-by-step process which starts from a CT scan and ends with a 3D organ model that it suitable for experimentation.

State of the Art

The main focus of this study is reproducing a model of the left ventricle. The first step is to obtain a CT scan which is suitable and reliable. It has to contain a clear scan of the heart with a small slice thickness, appropriate intravenous contrast, and low noise. The CT scan consists of a series

of DICOM (Digital Imaging and Communications in Medicine) images which need to be transformed into a mesh file. Therefore, it is necessary to segment the desired organ and convert it into a 3D model. To do that, the software Mimics by Materialize can be used. Each organ is segmented automatically and then manually to reach the most accurate surface possible. After segmentation of an organ is done on every single image contained in the CT scan, Mimics is able to convert the slices into 3D models (STL files) which need further modification. The end goal of this step is to create a rigid mold which is able to produce flexible models. To that end, 3-Matic by Materialize may be used to perform operations such as hollowing the model, removing any floating shells, filling any gaps, smoothing the surface, and much more. Most importantly, it can be used to divide the model into any desired shape. This shape must be easy to open and close in order to remove any model from it.

After the model is created, it is 3D printing. The 3D printing technique used is multi jet fusion using polyamide 12 (PA12) since multi jet fusion results in highly accurate surfaces and fine surface finishing.

The next step is to create a method which allows us to produce a flexible left ventricle model from the 3D printed model. The technique used in this study is rotational casting. A rotocaster consists of two frames, each rotating on a different axis such that any mold placed in its center is rotated bi-axially. The two frames are connected to a motor via a set of pulleys, gears, and belts which are able to translate the motor's rotational motion. In the center of the rotocaster, the mold must be mounted and rotated.

Liquid silicone must be poured into the mold which is then firmly closed. As the rotocaster rotates, the mold rotates as well, allowing the silicone inside it to spread uniformly across the walls. When the silicone has cured, the rotocater is stopped and a hollow, flexible and accurate 3D model of the left ventricle can be removed from the mold.

To produce an accurate model, many parameters need to be studied and optimized through experimentation. These are parameters such as the rotational speed of the rotocaster, the gear ratio between the two frames, the wall thickness of the produced model, the type of silicone,

and many more. Different grades of silicone must be tested in order to determine which one gives the best results.

Materials and Methods

A CT scan of the heart was obtained and the left ventricle, along with the other chambers, were segmented into 3D models. These models were further processed to produce the most appropriate molds. After creating several shapes to determine which mold would work best, the final mold was divided into two halves and connected via puzzle-like joints as shown in the figure below.

Figure 1: Left Ventricle Mold

The joints are connected to one half on one end, and the other half is subtracted from the second end. This allows the two halves to close firmly after silicone is poured in.

Next, a rotocaster was designed through many steps. Choosing the frame size depends on the type of models that will be produced by this rotocaster. Therefore, it was decided that and outer frame size of 600mm x 560mm and an inner frame size of 540mm x 500mm are enough. After determining the frame size, the different gear ratios required were calculated. Gear ratios can range from 1:1 up until 1:4. Next, the belts, bearings, bearing holders, supporting frames, clamps, and all the other components were studied and assembled on SolidWorks.

When all the components are decided upon, the torque required may be calculated in order to choose an appropriate motor that is able to provide the force needed to smoothly rotate the rotocaster. The final design of the rotocaster can be seen in the figure below.
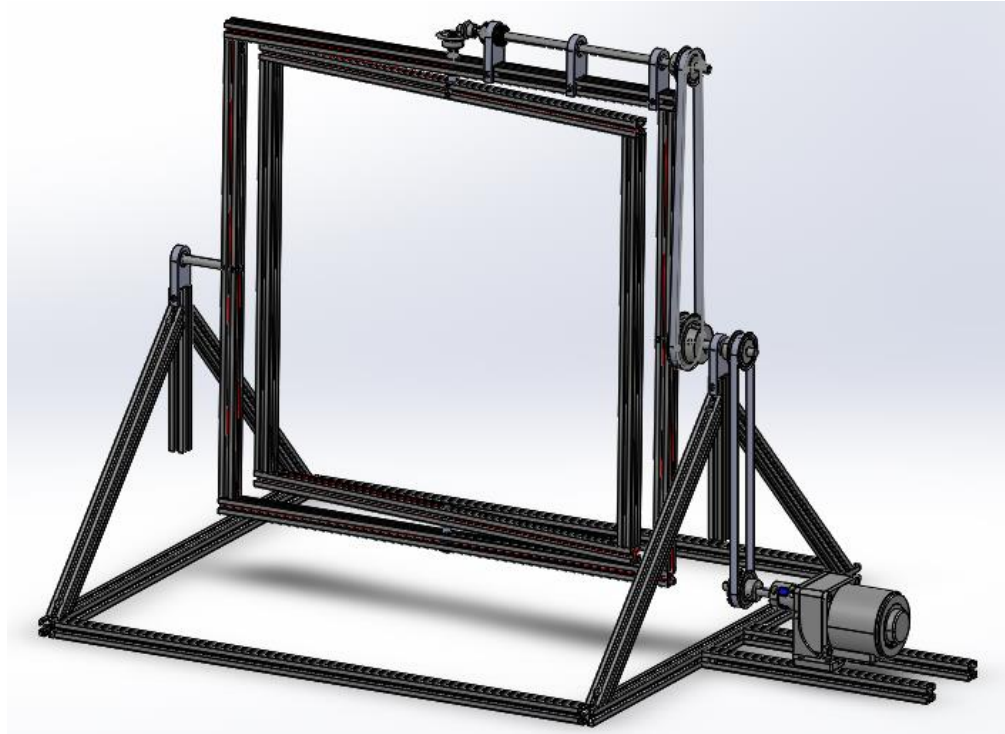
Figure 2: Rotocaster

The rotocaster then assembled and ready to work.

The different grades of silicone chosen for testing are then experimented on. Each experiment involved changing a single parameter. This parameter can be the type of silicone, the gear ratio, the rotational speed, the type of release agent, or the wall thickness.

When the desired wall thickness is chosen, the volume needed is measured and poured into the mold. Next, the appropriate gear ratio is setup on the rotocaster and the rotational speed is fixed. The rotocaster is allowed to rotate constantly for four hours until the silicone cures. The mold is then removed from the rotocaster and opened. With the help of release agent sprayed on the mold before pouring in the silicone, as well as the help of oil or soap water to remove the silicone model, the silicone model is then detached from the mold. The model is tested for any gaps and accumulations afterwards. Four different tests were done, each giving different results.

Results and Discussion

The results from the different experiments were studied and compared in order to formulate the best combination of parameters required to produce the silicone models.

It can be seen from the results that when a thicker silicone is used, accumulations can be found in narrow passages and area. In addition, a thicker silicone requires a lower rotational speed to allow the material enough time to spread evenly across the surface. In contrast, a thinner silicone was able to reach all the areas and required a higher rotational speed since slowing down the rotation causes the silicone to drip between opposite sides.

Using a larger wall thickness causes the loss of detail reproduction and is highly advised against. In case a thick wall is required, a thin wall may be used to create the model in the rotocaster and reproduce the highest details possible, and then extra silicone layers may be brushed on the outer surface where details are unimportant.

It can also be seen that the choice of release agent significantly affects our ability to be able to remove the silicone models without any tears. In the future, several other shapes and fittings may be used and are suggested in this report.

Conclusion

In conclusion, it can be seen from this study that the fabrication of 3D models of organs for experimentation is a very feasible topic. Starting from a CT scan, it is possible to create highly accurate models which can be used to test carbon dioxide catheters. With the correct combination of the parameters discussed, and with the help of imaging processing techniques and 3D printing, rotational casting has the capability to become a standard method in creating 3D flexible models suitable for experimentation.

I.   Introduction

During open heart surgery, blood is subjected to the gases of the operative field which could result in embolization after the surgery if deairing is not performed sufficiently. Embolization occurs when gas bubbles block a blood vessel, resulting in its occlusion. For example, it can result in infarctions if the coronary circulation is blocked, and neurocognitive impairments in the case of cerebral emboli. Deairing of the cardiac chambers was previously performed by several methods such as puncturing the left ventricle or the ascending aorta, ventilation, and needle aspiration; however, residual air in the cavities cannot be completely eliminated through these methods and results in central or peripheral organ gas embolization. To solve the problem of deairing, air in the operative field is replaced by CO_2 since it is more than 25 times more soluble than air in blood at ambient temperature. In addition, carbon dioxide has a higher density than air, and will displace air through the forces of gravity to take its place in the cavities. This process is called 'Carbon Dioxide Field Flooding' [1,2,3]. It has been shown that flooding the surgical field with carbon dioxide reduces the occurrence of emboli by 85% [4].

Air contains nitrogen, which is highly insoluble in blood, making it the main reason behind embolization. The solubility of carbon dioxide in blood is much higher than that of nitrogen and can significantly reduce any risks. The relative density of carbon dioxide to air is 1.5:1; therefore, it is able to displace air by gravity alone.

Gas	Gas Solubility Coefficients at 37-38°C
Nitrogen N_2	0.147
Oxygen O_2	0.027
Carbon Dioxide CO_2	4.0

Table 1: Gas Solubility in Blood [5]

With the emergence of minimally invasive cardiac surgery, carbon dioxide must be administered using different maneuvers which use smaller devices such as catheters. Many factors play a role

in determining the sufficient carbon dioxide flooding: the volume of the cavity, the carbon dioxide flow, the number of gas openings into the cavity, the type of device, the diameter of the openings, the position of the flooding device, the presence of suction, and any present movements. To test all of these parameters, an appropriate setup must be created.

The aim of this study was to create an appropriate setup which allows us to test the efficiency of different catheter designs and study the effects of different factors that influence the deairing process, such as carbon dioxide flowrates and access points.

To create such a setup, we proceeded by using image processing techniques to create three-dimensional CAD models of the left ventricle from medical CT scans. This model was further processed into different molds with different shapes, sizes, filling techniques, and joining mechanisms. Next, we used 3D printing to construct a hollow, solid model of the left ventricle molds which were designed. However, to test the efficiency of the CO_2 catheters, the left ventricle model must be able to mimic the behavior of a real organ. Therefore, we cannot use a solid model of the left ventricle; we must produce a hollow model with sufficient flexibility.

To construct any hollow, closed model using a flexible material, rotational casting was used. A rotational casting machine was designed, constructed, and tested to produce several models. Silicone was poured into the mold and mounted onto the rotational casting machine. Different grades of silicones were tested to produce models with various flexibility. Silicone was also chosen due to its transparency since it could allow us to observe the CO_2 flow inside the left ventricle.

Different factors were tested on the rotational casting machine to determine the most appropriate setting. Our aim was to produce a hollow, flexible model with a uniform wall thickness and without any tears that is also able to mimic the details of the inner wall of the left ventricle to the highest extent. We tested factors such as the rotational speed of the rotational casting machine, the gear ratio to change the rotation along different axes, the type of silicone, the wall thickness of the resulting model, and many more.

The results of each test were recorded in order to choose the most appropriate setting to produce a model of the left ventricle that is reliable for experimental procedures.

II. State of the Art

To create a 3D silicone model of the left ventricle, we proceeded by converting medical CT scans of the human heart into 3D printed molds, designing and constructing a rotational caster, and finally testing different grades of silicone to fabricate the models.

This section includes all the study and research done to choose the best methods required to carry out the methodology.

i) The Fabrication of 3D Printed Left Ventricle Molds from CT Scans

Choice of CT Scan – Over the past few decades, medical imaging has evolved drastically with the emergence of Magnetic Resonance Imaging (MRI) and Computed Tomography (CT). Three dimensional imaging data with a very high resolution can now be acquired easily, and 3D printing allows their visualization for several purposes [6].

Many 3D image acquisition systems may be used to form models that are suitable for 3D printing; however, not all of these systems provide models with good resolutions. The data most suited for 3D printing must be isotropic in order to result in accurate models [7]. A CT scan consists of a series of images or slices spaced out evenly, resulting in an isotropic dataset. Therefore, a CT scan is a form of 3D image acquisition system which can be used to form a mesh or a model that is suitable for 3D printing.

The quality of the 3D printed model depends on the quality of the data; therefore, it is important to choose a CT scan with desirable properties. Many parameters must be taken into consideration while deciding on a CT scan, such as the image slice thickness. The smaller the slice thickness, the higher the resolution of the 3D model obtained from it. It is recommended to use a slice thickness of 1mm or lower for the purposes of 3D printing [8]. Since the main goal is to capture the heart chambers, another important parameter is the presence of intravenous contrast. Intravenous contrast mixed with blood causes it to turn white in CT scans, allowing us

to separate any organ through which blood passes from any background tissue. It is also important to take into consideration the contrast timing since the contrast will flow through the blood vessels and reach different organs at different timings. The last parameter to consider is the reconstruction kernel, which involves a trade-off because a sharper kernel results in a higher resolution, but also higher noise [9]. Thus, a sharper kernel results in clearer images with distinct edges; however, the higher noise requires manual segmentation. A softer kernel results in the loss of details but facilitates automatic segmentation.

Segmentation – CT scans are usually saved as DICOM (Digital Imaging and Communications in Medicine) files. After obtaining these DICOM files, the next step is to convert them into a mesh representing the outer surface of the organ to be 3D printed in a process called Image Segmentation.

Segmentation is used to separate regions of interest from other parts of the body by manually, automatically, or semi-automatically assigning contours or thresholds on each image. These contours are then interpolated and smoothed to form a 3D body [7]. The medical image processing software which was chosen to be used for the segmentation process is Mimics by Materialize.

Different methods of segmentation exist. Manual segmentation requires the most effort and time but results in models with well-defined boundaries. Automatic segmentation is the fastest method but poorly defines boundaries of organs and results in inaccurate models. The most commonly used method is the semi-automatic segmentation method in which a seed point is required to automatically segment most of the region, followed by some manual modifications at the boundaries [10].

The Dynamic Region Grow tool in Mimics has proven to be very useful in segmenting blood vessels. Without defining any thresholds, a seed point is chosen and is grown to reach all the connected points with the same intensity value. This tool is enough to segment the heart as a whole; however, to segment the different chambers, further manual modifications are required. To segment the left ventricle, a mask must be created in which any connections with other

chambers must be eliminated and any missing boundaries must be included in the mask. This procedure must be repeated for each image, making it a long process which results in the most accurate models.

Creating an STL File – The segmented heart chambers may then be exported as STL files which still need further modifications. Although segmentation allows us to separate the desired chambers, it results in solid organs which need to be hollowed. Since segmentation considers the blood, the resulting chamber's outer surface is actually the chamber's inner wall in reality. Using 3-Matic by Materialize, we are able to create a hollow chamber with a uniform wall thickness and an accurate inner surface.

3-Matic also allows us to perform different operations such as closing any holes in the surface, smoothing it out where required, and removing any floating shells. In addition, it allowed us to divide the model into different parts in order to create an assembly which can be opened and closed tightly when needed.

All of these operations can result in a model that is ready for 3D printing. If further modifications are needed to reduce the resolution, the image processing software, Meshmixer, can also be used.

3D Printing – 3D printing, also known as additive manufacturing, is a manufacturing method which uses a variety of materials and deposits them in two dimensional layers, one on top of the other, to produce three dimensional objects [11]. Advancements in 3D printers and printing materials have allowed it to be used in the medical field for several purposes such as surgical planning, prostheses, medical education and training, medical research, and many more [12].

The most commonly used 3D printing techniques for medical purposes are Fused Deposition Modeling (FDM), Stereolithography (SLA), Multi Jet Fusion (MJF), and Selective Laser Sintering (SLS) [13].

Fused Deposition Modeling (FDM) involves melting filamentous thermoplastic materials and extruding this material through the tip of a nozzle of the 3D printer [14]. It uses modeling material and support material which are fed through the extrusion nozzle onto a platform. The nozzle melts the filaments onto the base one layer at a time, such that both the nozzle and the platform are controlled by a computer [15]. The thin layers then cool and harden, creating tight bonds between them. It has a relatively low resolution and produces models with very rough surfaces.

Stereolithography (SLA) is a technique which involves the polymerization of a photopolymer by means of illumination (e.g., laser or projector) [16]. The resin is poured into a tank and a built platform is lowered into the resin, leaving a thin layer of liquid between the platform and the bottom layer of the tank. The light source is then directed to draw a cross section of the 3D model and selectively cure the liquid resin into hardened plastic. The process is repeated in several thin, consecutive layers [17]. It results in highly smooth surfaces and is ideal for printing hollow models without any support material.

Selective Laser Sintering (SLS) is the process in which a laser is used to bind powder plastic, ceramic, metal, or glass together [18]. The powder is preheated to a temperature below its melting point and placed in a thin layer across a platform. The laser then traces the cross section of the 3D model, allowing the particles to fuse together and form a solid part. The need for support material is eliminated since the unfused powder can support the body. The process is then repeated for each layer [19]. It results in rough surfaces and requires substantial post processing.

Multi Jet Fusion (MJF) uses thermoplastic-based powder, fusion agents, and detailing agents. Fusing agents are jetted selectively, depending on where the particles need to bind together. A detailing agent is used to define the boundaries [20]. This technique results in slightly rough surfaces; however, the surfaces can be smoothed with suitable finishing techniques.

The following table compares the advantages and disadvantages of the 3D printing techniques described above.

3D Printing Technique	Advantages	Disadvantages
Fused Deposition Modeling	- Produces parts with high strength. - Low cost	- Slow printing process - Poor surface finishing
Stereolithography	- Produces very fine details. - Results in a smooth surface finishing	- Results in weak models - Susceptible to light and heat
Selective Laser Sintering	- Produces strong and complex parts. - Build large volumes.	- Grainy surface finishing
Multi Jet Fusion	- Uses a variety of materials - High accuracy - Fine surface finishing	- Low strength - Susceptible to heat and sunlight.

Table 2: Advantages and Disadvantages of 3D Printing Techniques [21]

ii)   Designing and Assembling a Rotational Caster

Rotational casting is the process in which a liquid is poured into a mold and rotated bi-axially to create a hollow model with a uniform wall thickness [22]. The required mold needs to be divided into two halves at least, such that the mold is opened, a desired amount of the liquid is poured into one half, after which the mold is tightly closed. The mold is then mounted onto the rotational caster which rotates automatically and bi-axially. This allows the liquid to spread evenly across the surface, resulting in a uniform wall thickness. After material curing is reached, the mold is taken out, opened, and the model is removed.

The advantages of rotational casting lie in its ability to produce versatile designs made from flexible materials, which can be both watertight and hollow. It also has the ability to produce the smallest of details in models.

To design a rotational caster, many factors need to be taken into consideration such as the RPM. When using materials like silicone which take hours to cure, if the RPM is too slow, we risk having the material drip from side to side; whereas, if the RPM is too high, we risk having an uneven distribution of the material. in some cases, the RPM can vary throughout the process. Another important factor is the gear ratio which determines the difference in the speed of rotation between the two axes of rotation. Different shapes will require different ratios to allow the molding material to spread uniformly.

Designing a rotocaster requires the design of several components including gears, belts, shafts, bearing holders, and many more. The first step is choosing an appropriate frame size that can fit the molds.

To prevent any vibrations in the rotocaster, the motor must be placed externally and connected via pulleys and gears to transfer its rotary motion to the inner and outer frames. The motor shaft must be connected to another shaft via a clamp type shaft collar to extend its length. A pulley is connected to the second shaft and its motion is transmitted to another pulley via a belt. The second pulley drives the external frame mainly. To calculate the length of the belt, the following equation was used:

$$L = 2C + \pi \left(\frac{D_2 + D_1}{2}\right) + \left(\frac{D_2 + D_1}{4C}\right)^2 \quad such\ that \begin{cases} C: center\ length\ between\ 2\ pulleys \\ D_1: pitch\ diameter\ of\ first\ pulley \\ D_2: pitch\ diameter\ of\ second\ pulley \end{cases}$$

To transfer the motion to the internal frame, the second pulley is connected to a third pulley via a shaft. The third pulley is fixed to the frames through the use of pins to prevent it from rotating. The third pulley must then be connected to a rotating pulley through a belt, and then to a set of bevel gears through a shaft.

Bevel gears are used to transfer the rotary motion between two intersecting shafts. The shaft from the bevel gears is fixed to the inner frame, giving it its rotary motion. Bevel gears must be assembled in a specific way to ensure smooth running and optimum load distribution between the gears, without binding and excessive backlash. To guarantee that, the mounting distance, which is the distance from a surface on the front or back of one gear to the centerline of the mating gear, must be calculated. If the mounting distance is less than the distance specified, excessive backlash may occur. In addition, the gears must be rigidly supported to be able to handle the loads. This can be done by placing springs which always push the gears towards each other [23].

Bearings are used to allow shafts to pass through the frames with minimal friction.

To choose the motor, the weight of each component is found, and the torque required to provide the rotation is calculated. Based on these findings, a motor is chosen. Firstly, a mass equal to that

of the pulleys, belt, bevel gears, and shaft will be added to the opposite side of the outer frame to maintain symmetry and keep the center of mass in the middle. The torque is then calculated based on the weights of all the components, in addition to a safety factor.

iii)   Materials Research

The human heart is a soft, flexible tissue which allows a pulsatile flow. It cannot be modeled using rigid materials which cannot mimic the contraction and relaxation phases of the heart. To mimic the heart's behavior as closely as possible, the elastomeric properties of silicone have proven to be of great advantage. Many studies made to produce soft artificial hearts have used silicone due to its ability to mimic the physiologic flow inside the heart [24].

The final purpose of this study is to produce a model of the left ventricle that is suitable for experimentation. One advantage which silicone can offer is its transparency which makes it feasible to observe flows inside of it.

The elastic modulus of the left ventricular muscle is between 0.007 MPa and 0.11 MPa during the diastolic phase, and between 0.027 MPa and 0.4 MPa during the systolic phase [24]. Even though the elastic modulus of silicones is generally higher than that of the left ventricular muscle, it is still a significant improvement from other materials which have been used and it offers a higher physiological reproducibility.

The table below summarizes the mechanical properties of the silicones that will be tested in this study.

Material	Tensile Strength [MPa]	Elastic Modulus [MPa]	Elongation at Break (%)
Dragon Skin 20 Silicone	3.8	0.34	620
Eurosil 33 Silicone	4.7	2	430
Dragon Skin 10 Silicone	3.3	0.15	1000

Table 3: Mechanical Properties of Silicones [25,26]

III.   Materials and Methods

The following section discusses in detail the procedure that was followed throughout this study to produce artificial silicone hearts, based on the literature review.

i)   The Fabrication of 3D Printed Left Ventricle Molds from CT Scans

To proceed with this step, it is first required to obtain a CT scan of the heart with parameters that are suitable for 3D printing later on. Each CT scan was checked for any foreign material before proceeding with the rest.

The CT scan chosen had the following parameters:

- Slice Thickness: 1.5 mm
- Pixel Spacing: 0.5859375 mm x 0.5859375 mm (512x512)
- Protocol: Gated CT scan of the thoracic aorta
- Study Date: 11/04/2005
- Patient's Age: 73 years old

The DICOM files were opened in Mimics in order to proceed with the segmentation procedure. To perform segmentation, the 'Dynamic Region Growing' tool, which combines thresholding and region growing in one step, was used. It is based on the connectivity of gray values within a specified range of seed points of our choosing. As we move the cursor to choose a seed point, the pixel value changes. Once we choose a seed point, it grows out to any connected voxels that are within the deviation of the chosen intensity value. By checking the option 'Multiple Layer', it includes all the layers in the dataset. We can also choose to fill in any holes.

This tool automatically creates a mask with a minimum and maximum threshold. However, it is not totally accurate. To fix this issue, each mask is then edited individually, and each image slice is manually modified to include only the chamber in question, separated from any other chamber and including its accurate boundaries. If any chamber was difficult to visualize, the contrast was manipulated until the entire boundary was clear.

After a mask is created, the 3D model may then be produced by using the 'Calculate Part from Mask' tool.

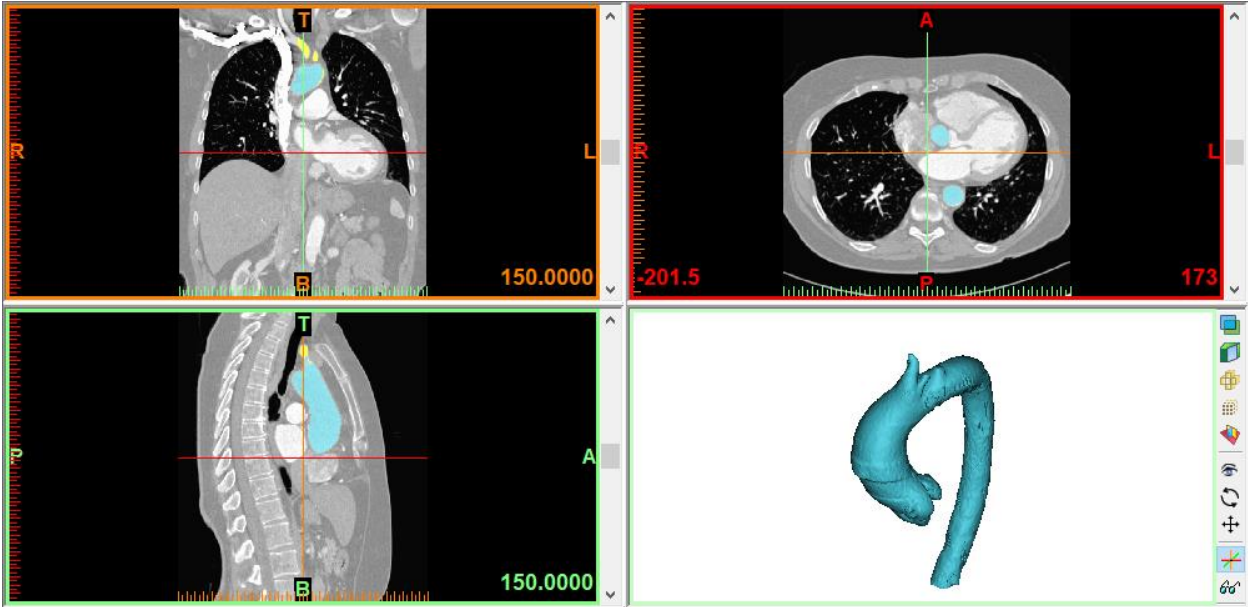The figures below demonstrate the results of the segmentation process.
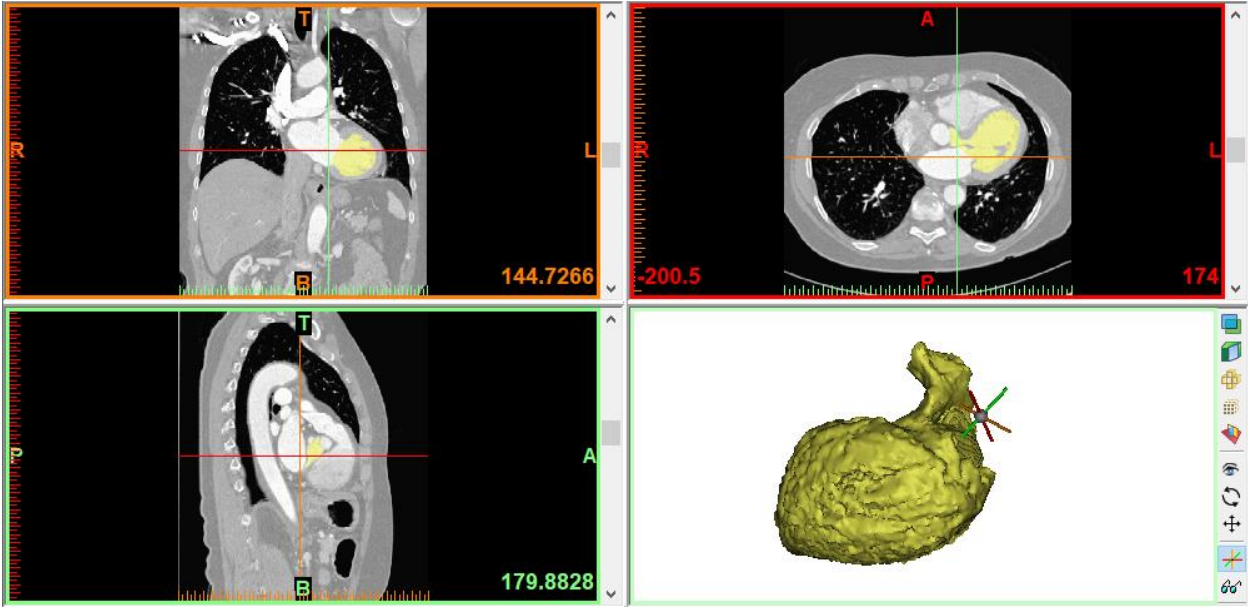

Figure 3: Segmentation of the Aorta
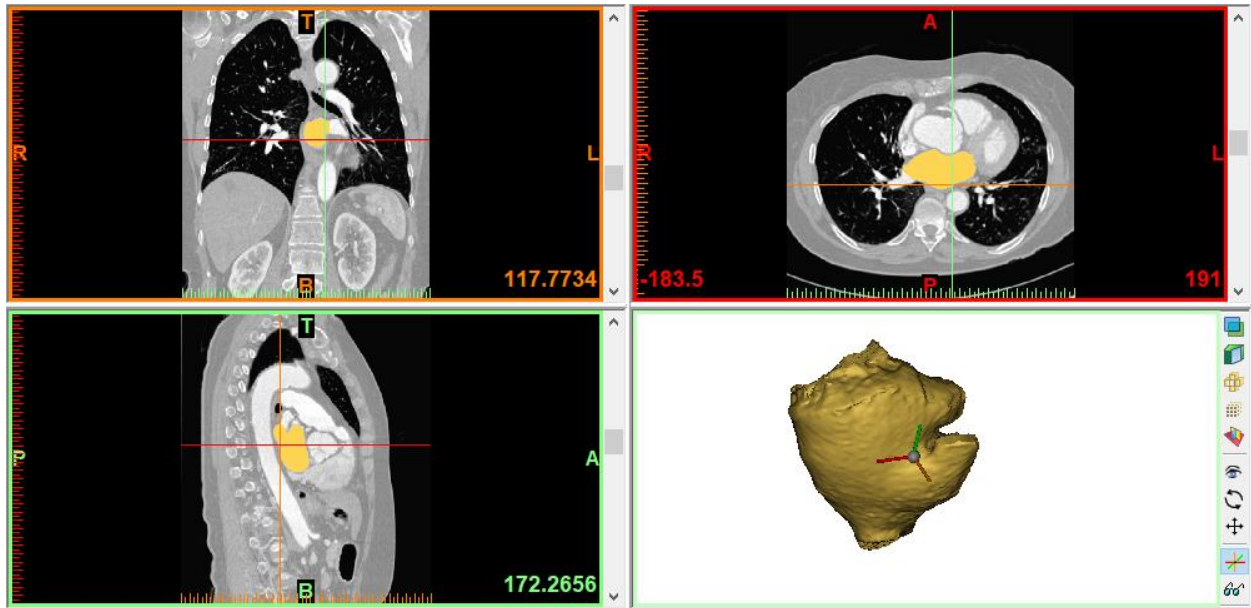

Figure 4: Segmentation of the Left Ventricle
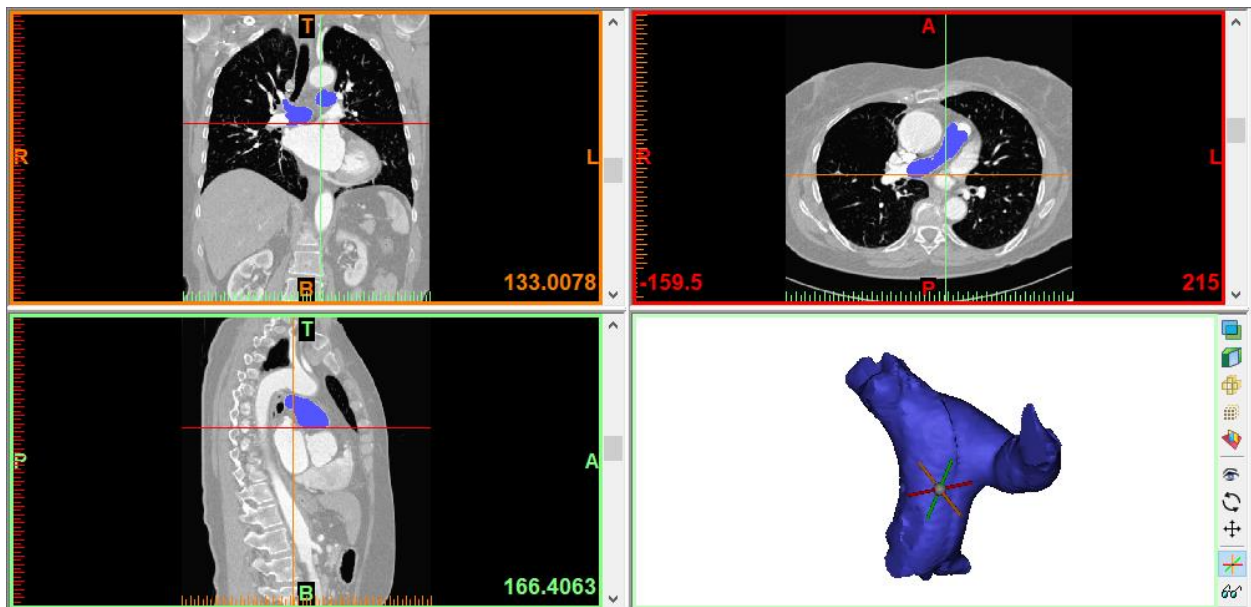
Figure 5: Segmentation of the Left Atrium

Figure 6: Segmentation of the Pulmonary Artery

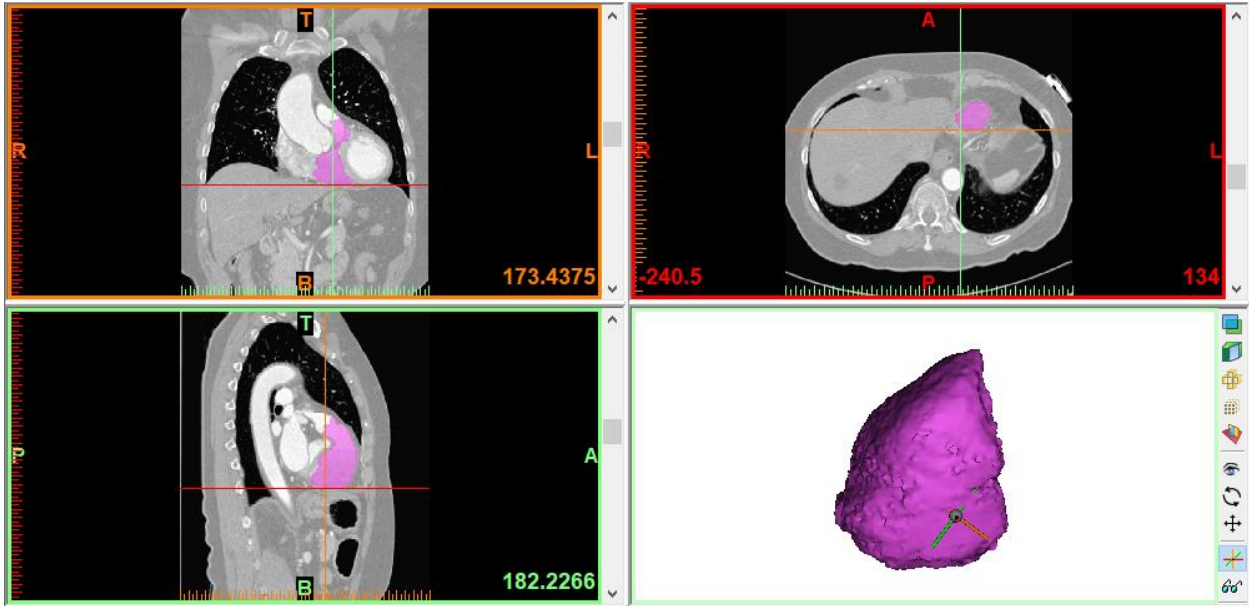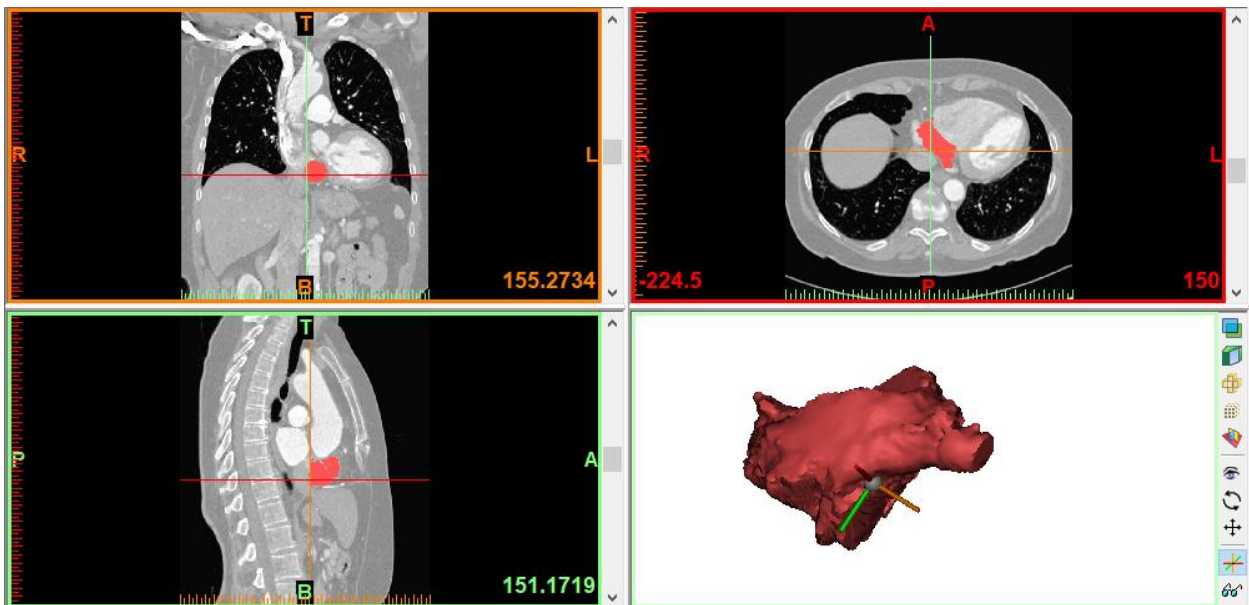*Figure 7: Segmentation of the Right Ventricle*

Figure 8: Segmentation of the Right Atrium

To segment the myocardium, we cannot use the same procedure because the boundaries are not as defined. To do that, we create a mask including all of the chambers (threshold 1) and a mask including all of the previously segmented chambers (threshold 2). The addition of all the

segmented masks can be done by using the 'Boolean Operations' tool. Next, threshold 2 is subtracted from threshold 1, leaving behind the myocardium.

The segmented myocardium, as well as other segmented structures, can be seen in the figures below.
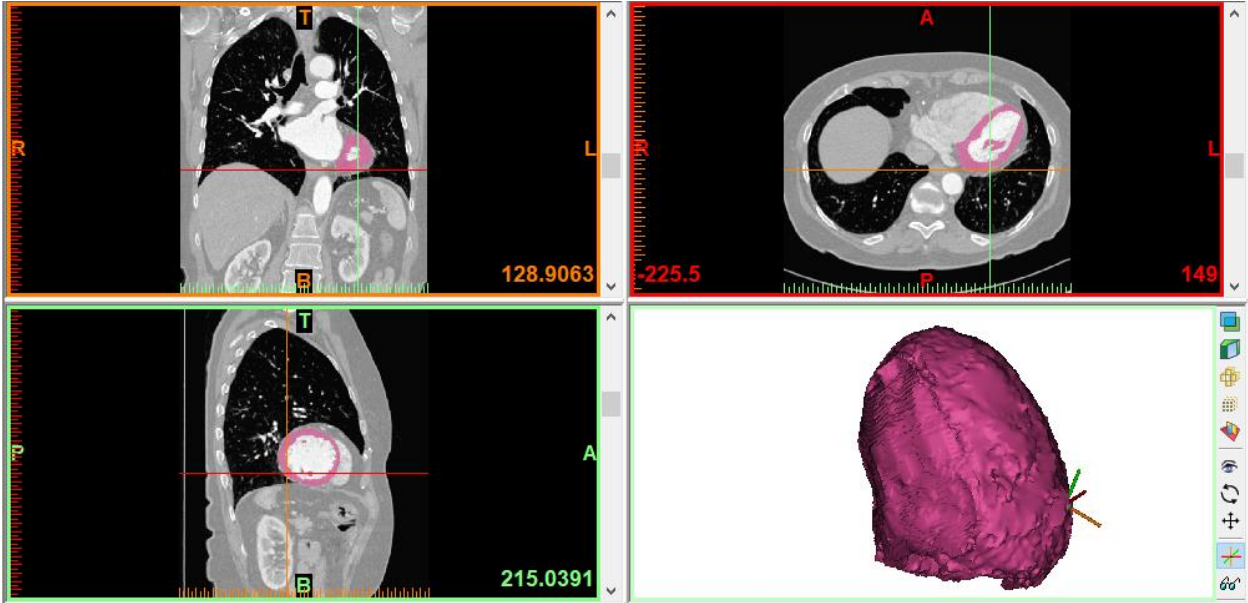

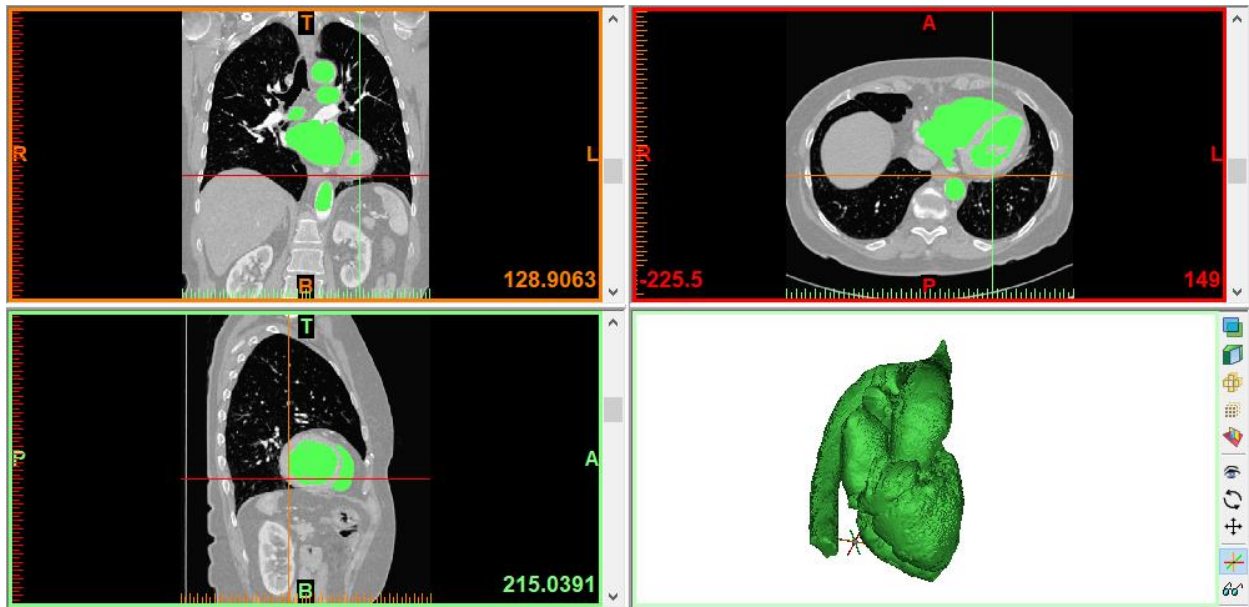*Figure 9: Segmentation of the Myocardium*
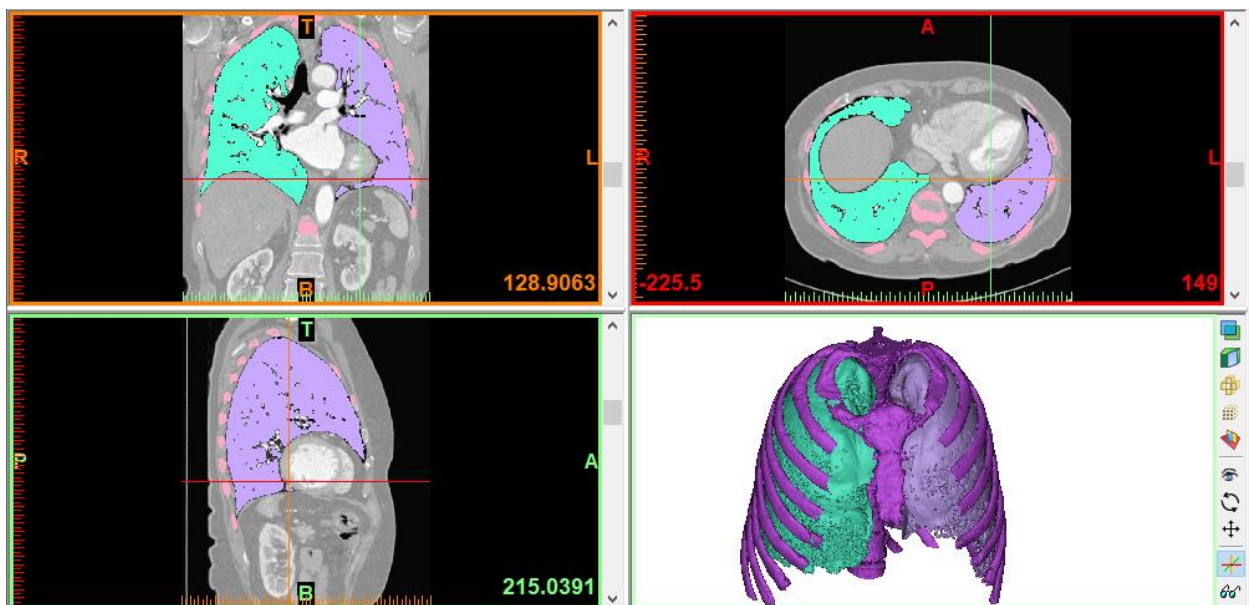
Figure 10: Segmentation of the Whole Heart

Figure 11: Segmentation of the Thorax, Left Lung, and Right Lung

The table below lists the maximum and minimum values of the threshold chosen for each segmentation process.

Structure	Minimum Threshold [HU]	Maximum Threshold [HU]
Aorta	260	620
Left Ventricle	226	560
Left Atrium	226	725
Pulmonary Artery	226	3071
Right Ventricle	75	3071
Right Atrium	100	3071
Myocardium	52	3071

Table 4: Threshold Values for Segmentation

After segmentation, each part is exported to 3-Matic, a post processing software for STL files. In 3-Matic, the first step is to perform a 'Wrap' operation which closes any holes on the surface, smoothens it out, and removes any internal shells in the model. It makes the model watertight and easily printable. The smallest detail value chosen was 0.5mm; therefore, any detail smaller than that will be lost.

The 'Wrap' operation is essential for several reasons. Any holes left in the model will result in the leakage of silicone from the mold. In addition, internal and floating shells cannot be 3D printed and need to be removed. Finally, smoothing out the surfaces makes removing the silicone mold easier and prevents any tears resulting from the material getting stuck in sharp edges.

Next, we need to transform the solid part into a hollow chamber using the 'Hollow' tool. The hollowing is performed to the outside so that the outer surface becomes the inner surface of our model. At this point, we need to give our model a uniform wall thickness. A thickness of 2mm was chosen for most of the designs as it provides enough rigidity.

To add the myocardium to the left ventricle, we perform a Boolean union operation and add it to the outer surface of the ventricle before hollowing it out.

Lastly, to transform the model into a usable mold, we must divide it into different parts that can be opened and firmly closed. Also, to mount this mold onto the rotational caster, we must add holes for inserts. Different configurations were designed for this purpose.

The first configuration, shown in the figures below, involves dividing the left ventricle into two parts, and aligning them using two rectangular slots. Two 15mm diameter cylinders were protruded to allow the insertion of two inserts of diameter 3.5mm and depth 4mm.
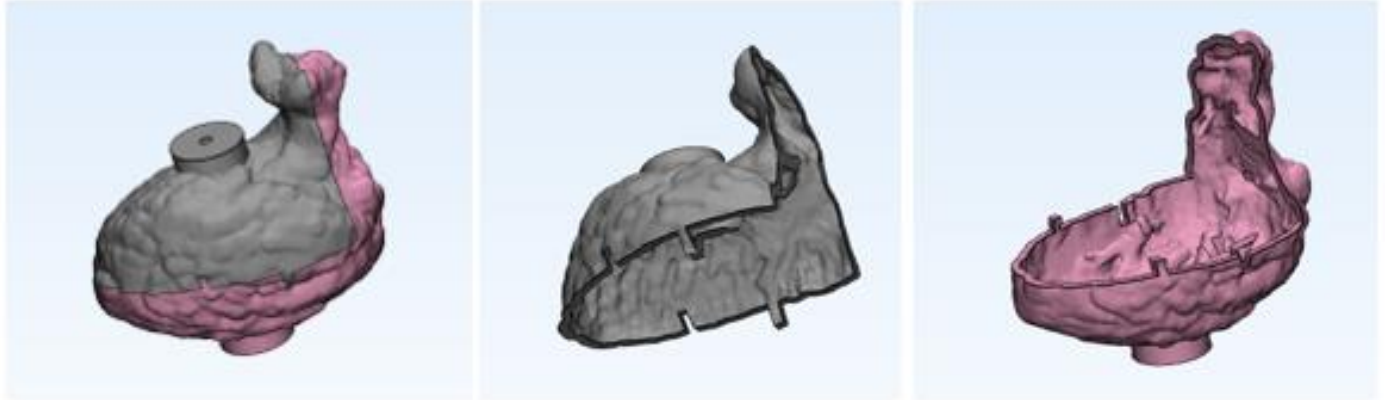
Figure 12: Left Ventricle Mold - Configuration #1

The second configuration has a different alignment mechanism. Three puzzle-like joints were added by extruding a rectangular shape and then subtracting the ventricle from it, making it a perfect fit. The cylinders were reduced to a 10mm diameter. In this configuration, the dividing cut was chosen differently to allow the reproduction of the papillary muscles.
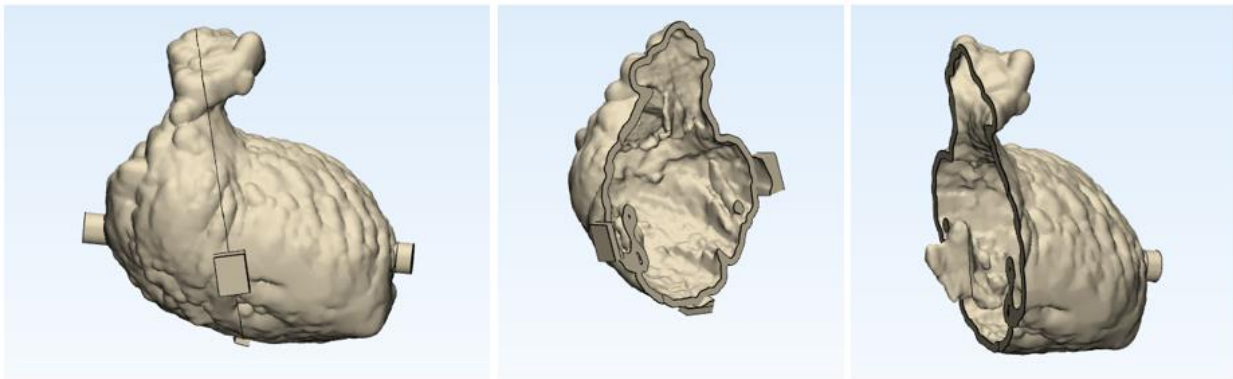
Figure 13: Left Ventricle Mold - Configuration #2

In the third configuration, the position of the tabs and insert cylinders was changed. In addition, the cylinders were transformed into conical shapes.
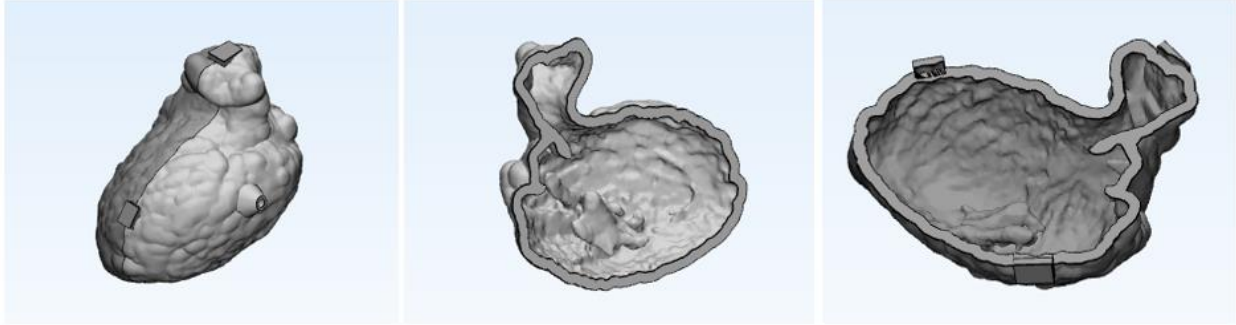
Figure 14: Left Ventricle Mold - Configuration #3

Finally, the second configuration was 3D printed by Multi Jet Fusion from polyamide 12 (PA 12) from RAPIDOBJECT GMBH. The resulting molds are shown in the figures below.

Figure 15: 3D Printed Mold of the Left Ventricle

ii)   Designing and Assembling a Rotational Caster

To create the artificial silicone left ventricle, silicone must be poured into the mold and rotated until it cures. Thus, we need to design and build a rotational caster. Most of the components used were ordered from MISUMI. A list of all the components used for the construction of the rotocaster and some technical drawings are included in Appendix A.

The first step is to construct a support frame which holds the rotating frames and connects them to the motor. The base of the support frame is 650mm x 740mm, and its height is 350mm.

Two bearing holders were designed and manufactured specifically for this rotational caster. They hold ball bearings through which a shaft connecting the inner frames to the motor will pass.
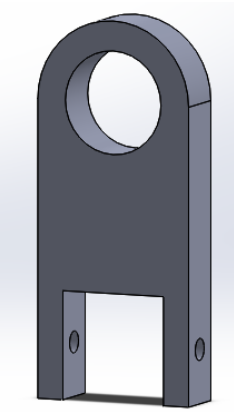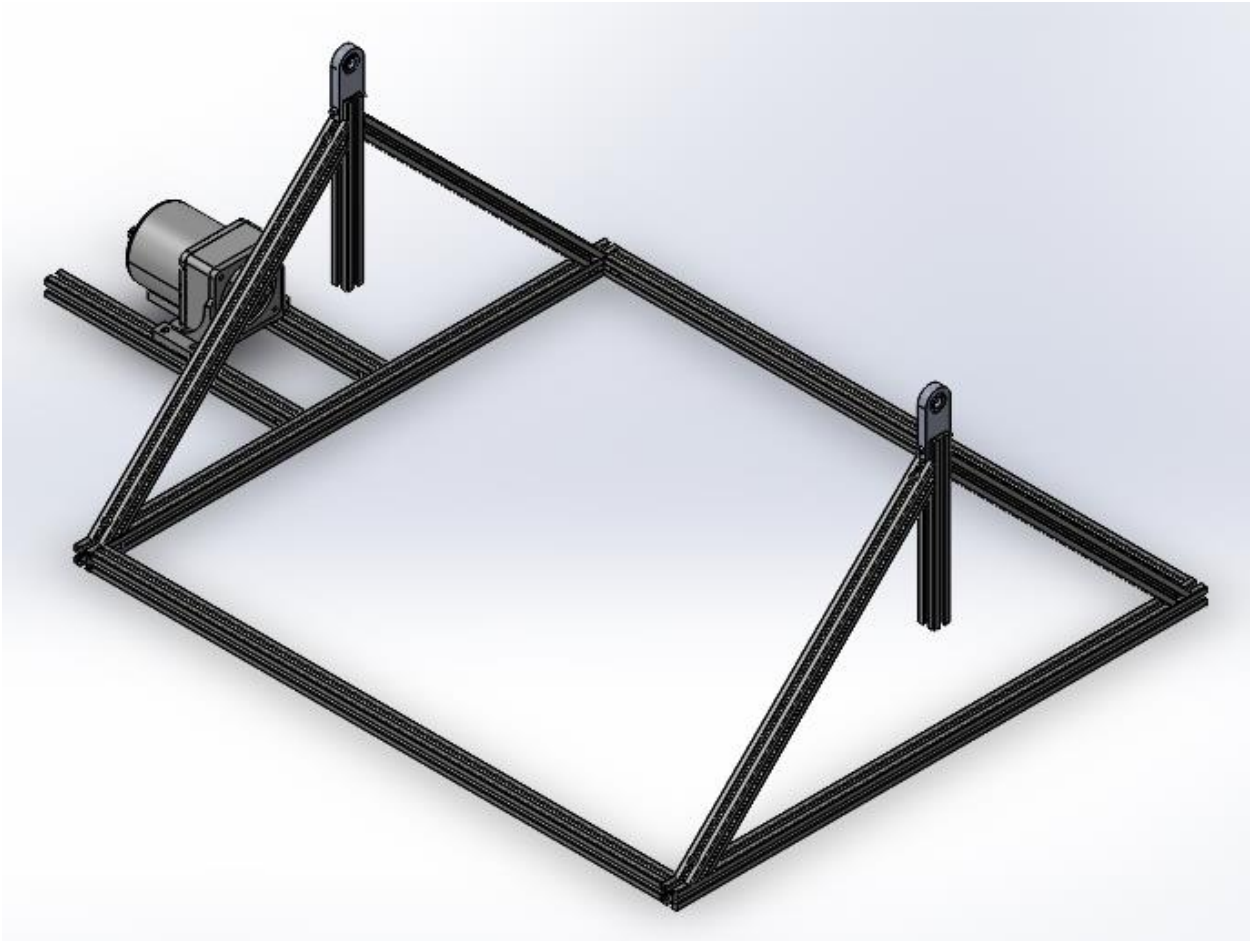

Figure 16: Ball Bearing Holder Design

*Figure 17: Rotational Caster Support Frame*

Next, the inner and outer frames of the rotocaster were assembled. In the outer frame, two shafts were fixed by drilling through them and through the frame itself and holding them together using spring pins. These shafts are used to connect the outer frame to the support frame through the bearings in the bearing holders. Two holes were also drilled to insert sleeve and flange bearings. These holes are used to connect the outer frame to the inner frame.
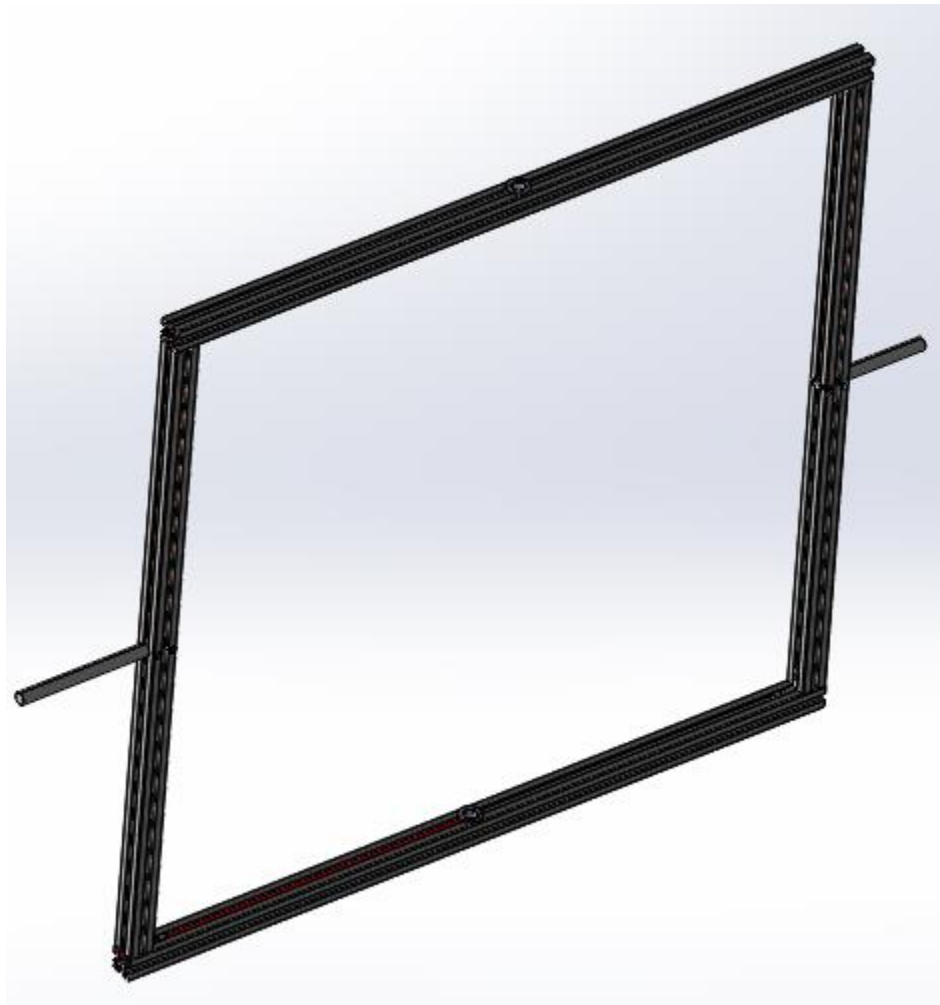
Figure 18: Outer Frame of the Rotational Caster

In the inner frame, one shaft was drilled into the frame to connect it to the outer frame through one of the bearings. This shaft will be connected to a gear mechanism mounted onto the outer

frame, which will transform the motion between them. Another shaft was inserted into the frame through bearings. It connects the inner frame to the outer frame and passes through the bearings inserted into the outer frame. This shaft is meant for alignment purposes.
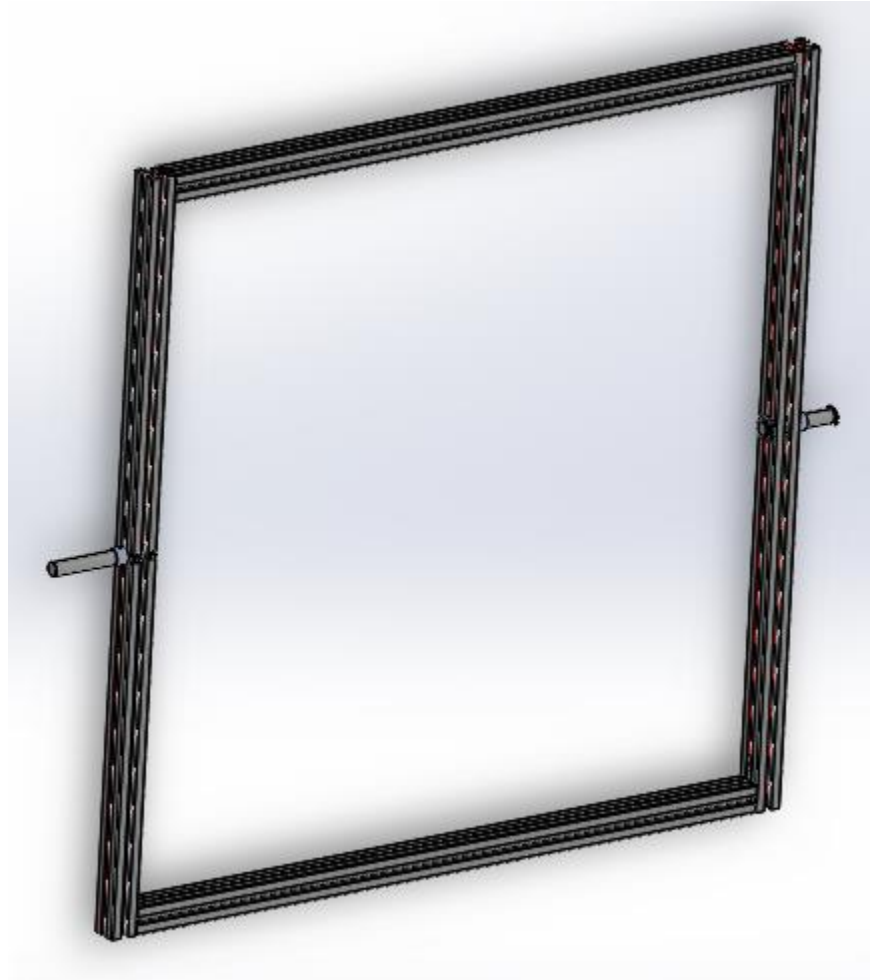
Figure 19: Inner Frame of the Rotational Caster

To create the required motion, a series of bevel gears, pulleys, and belts were used. The motor was connected to the main shaft through two pulleys and a belt. The main shaft is then connected, through a similar mechanism, to a shaft mounted onto the outer frame. This shaft is passed through bearings and bearing holders and ends with a bevel gear perpendicular to it. The bevel gear then engages with another bevel gear perpendicular to it and connected to the inner frame. Springs were used to make sure that the bevel gear remains in its position.
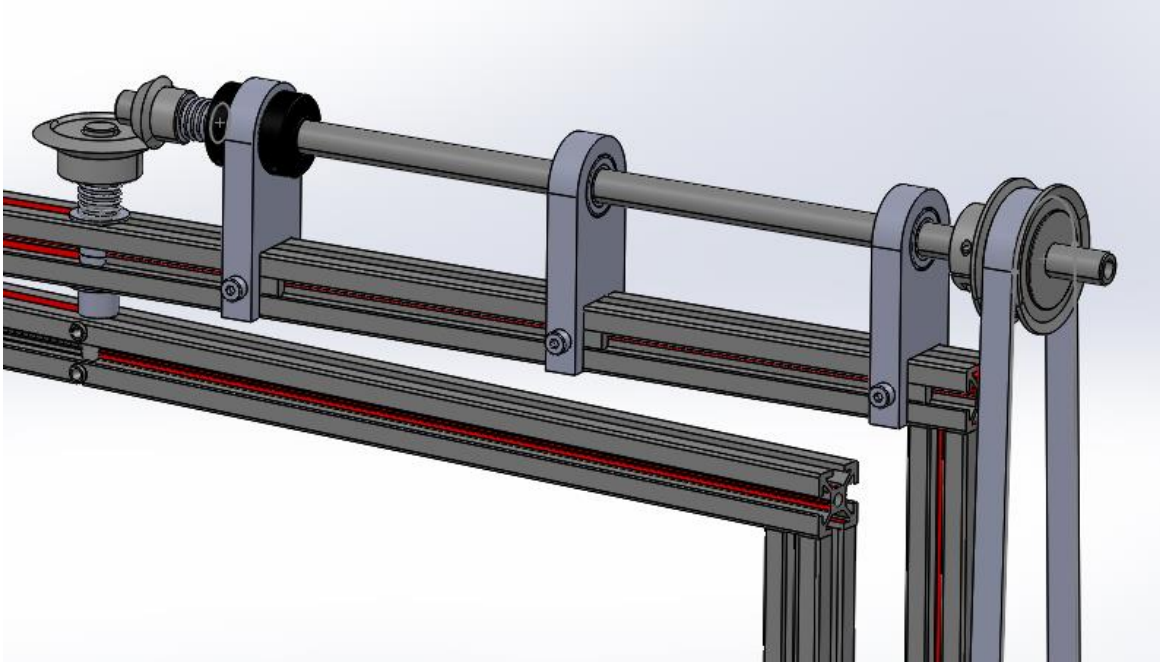
Figure 20: Motion Transmission Mechanism between Inner and Outer Frames
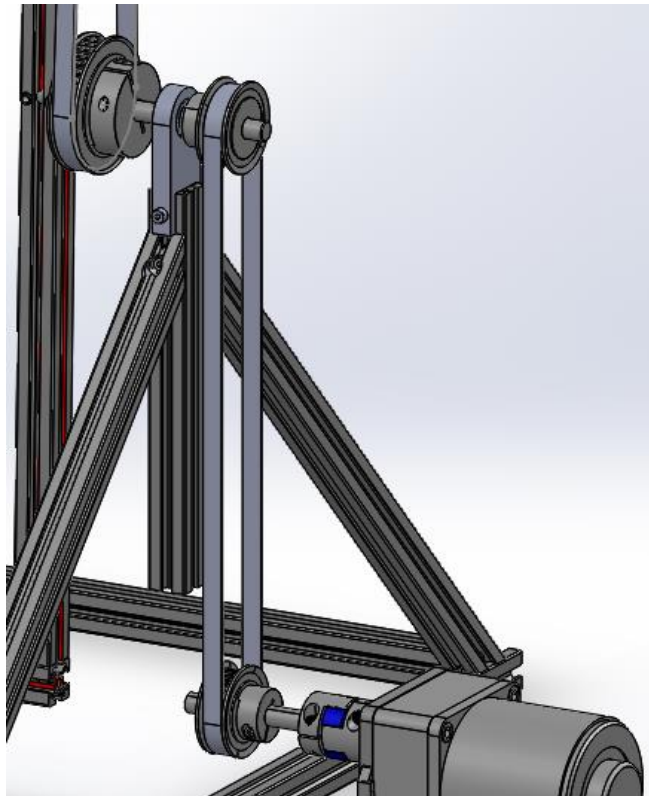

Figure 21: Motion Transmission between Motor and Frames

In this way, when the outer frame rotates about a horizontal line, the inner frame rotates about a line that is vertical with respect to the outer frame. This allows any mold mounted inside the rotational caster to rotate on all angles possible.
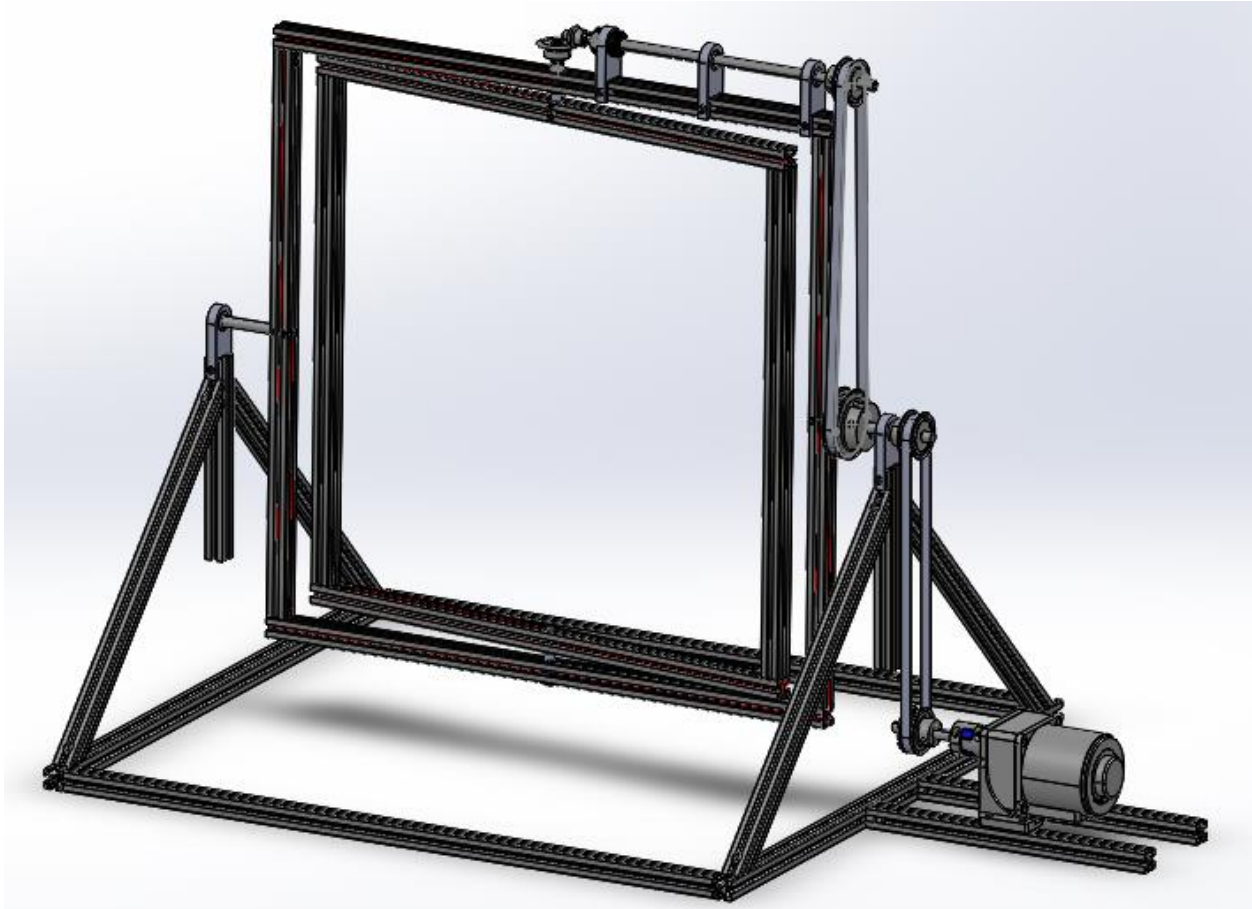
Figure 22: The Rotational Caster

If a gear ratio of 1:1 is used, the speed of rotation of the inner frame and outer frame will be the same. Changing the diameters of the gears and pulleys allows us to obtain different results.

The gear ratio can be calculated as the ratio of the diameters (D), number of teeth (N), rpm (ω), and torques (τ) of the two gears:

$$Gear\ Ratio = \frac{N_{Driven}}{N_{Driver}} = \frac{D_{Driven}}{D_{Driver}} = \frac{\tau_{Driven}}{\tau_{Driver}} = \frac{\omega_{Driver}}{\omega_{Driven}}$$

This formula was used to obtain the gears and pulleys required for a 1:1, 1:2, and 1:4 gear ratio.
Their values are shown in the figures below.

D=20 mm

D=40 mm

N=24 teeth

N=40 teeth

N=24 teeth

N=24 teeth

Figure 23: 1:1 Gear Ratio

D=30 mm

D=30 mm

N=40 teeth

N=40 teeth

N=24 teeth

N=24 teeth

Figure 24: 1:2 Gear Ratio

D=40 mm

D=20 mm

N=24 teeth

N=40 teeth

N=24 teeth

N=24 teeth
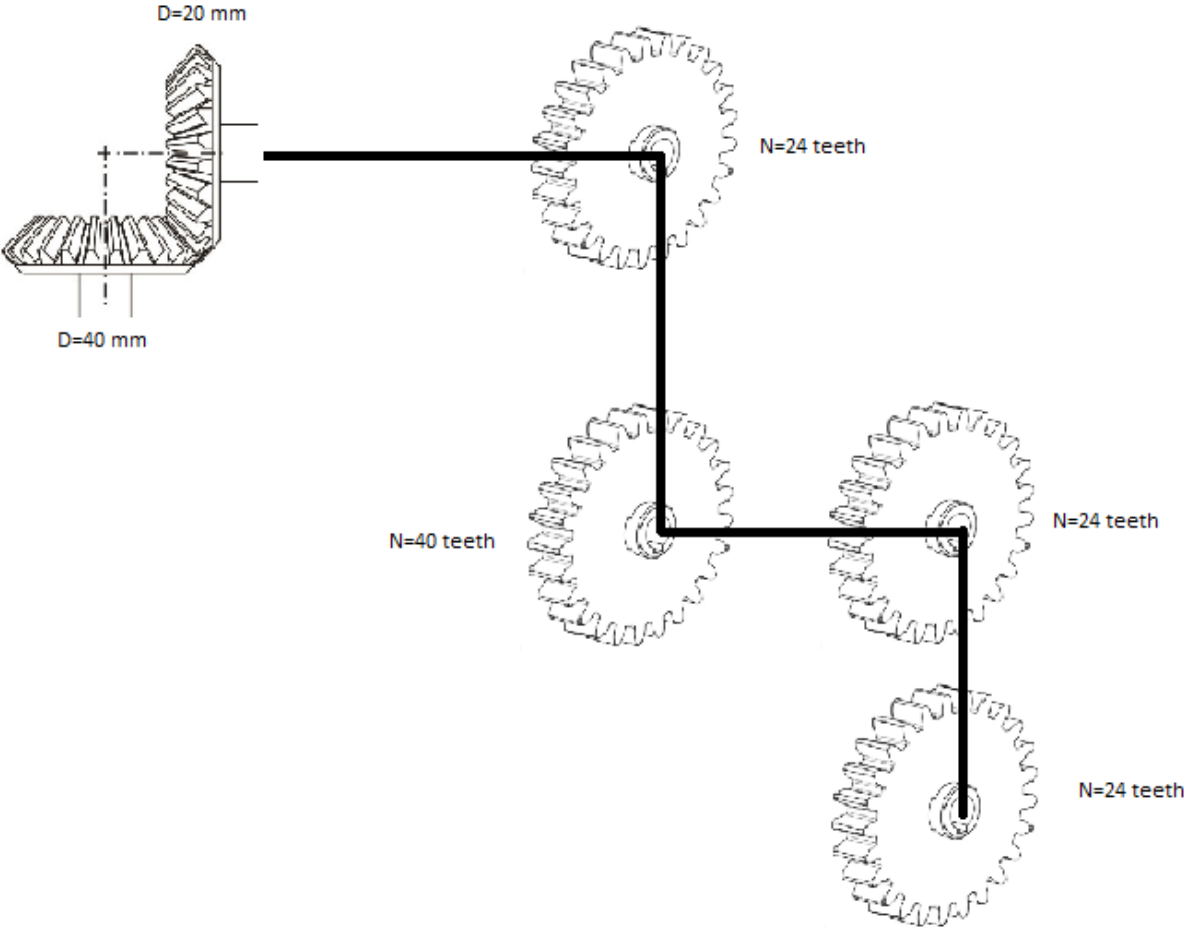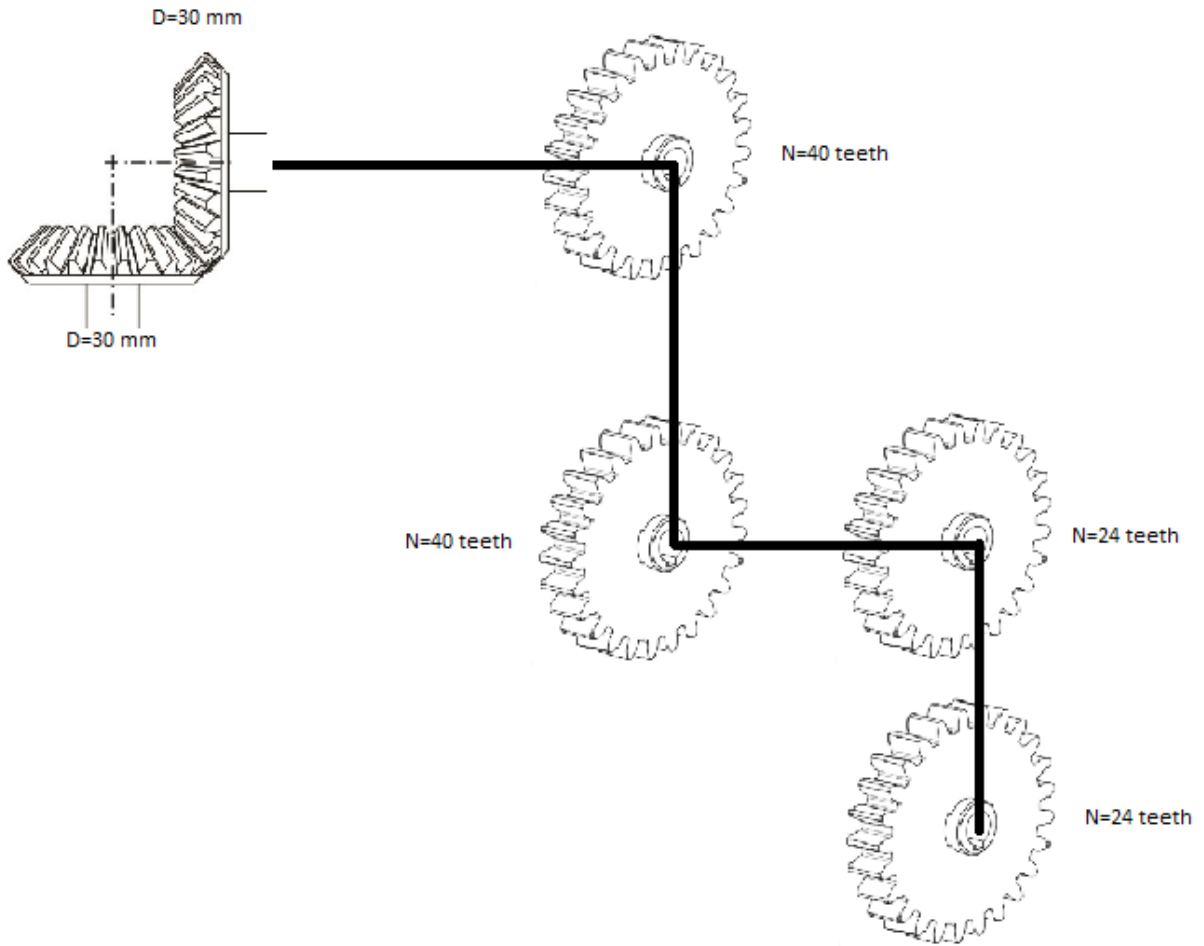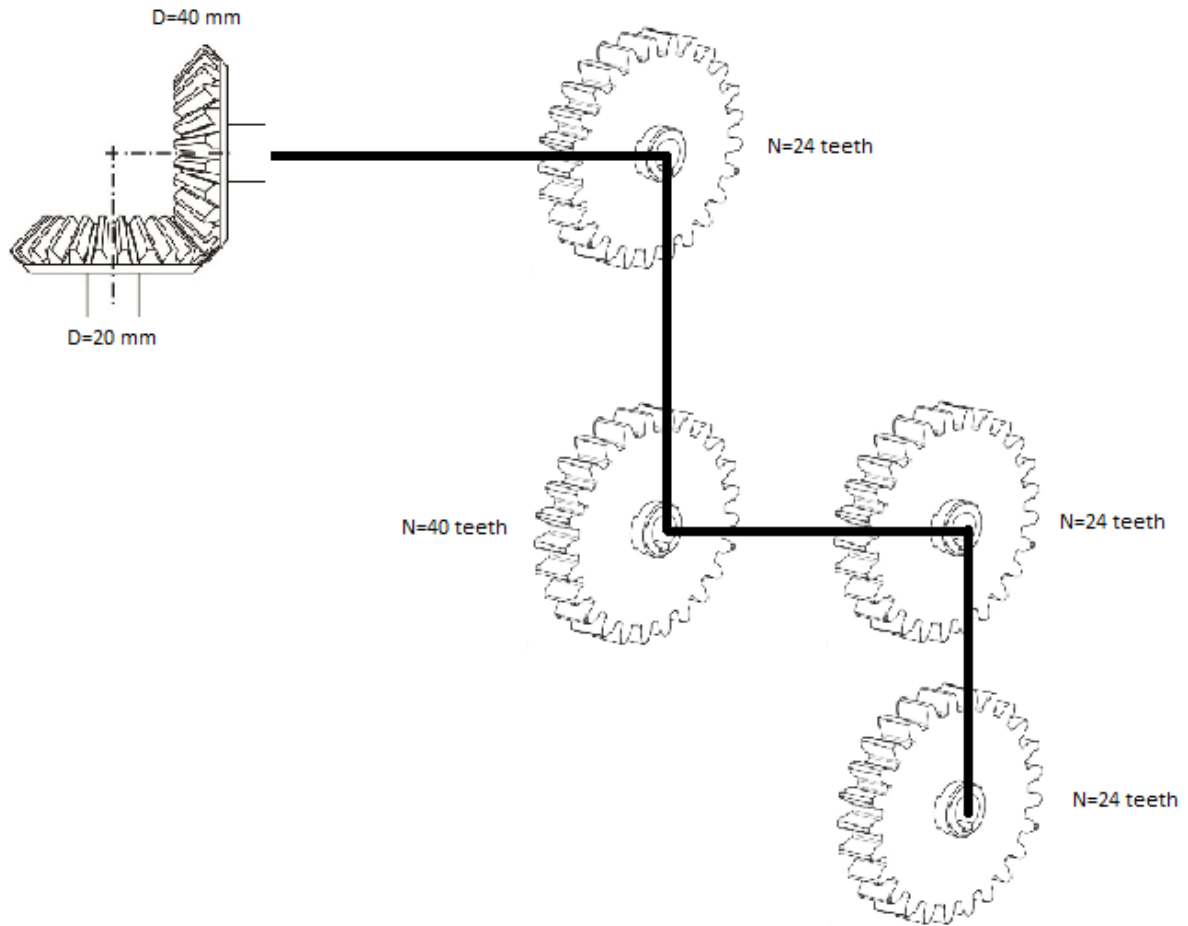
Figure 25: 1:4 Gear Ratio

Finally, to place the mold inside the rotocaster, inserts were 3D printed and glued onto the extruded cylinders of the mold. Then, the mold was screwed onto two short frames connected to the inner frame.
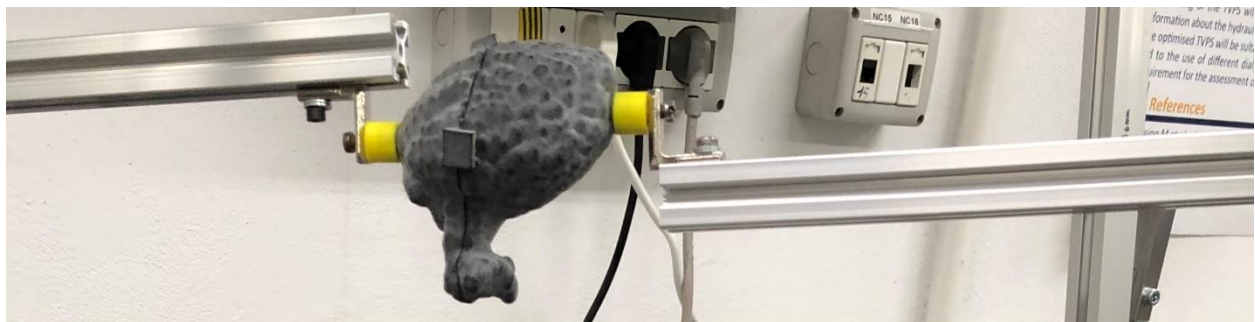
Figure 26: Mounting Method for the Mold

The final design is shown in the figure below.
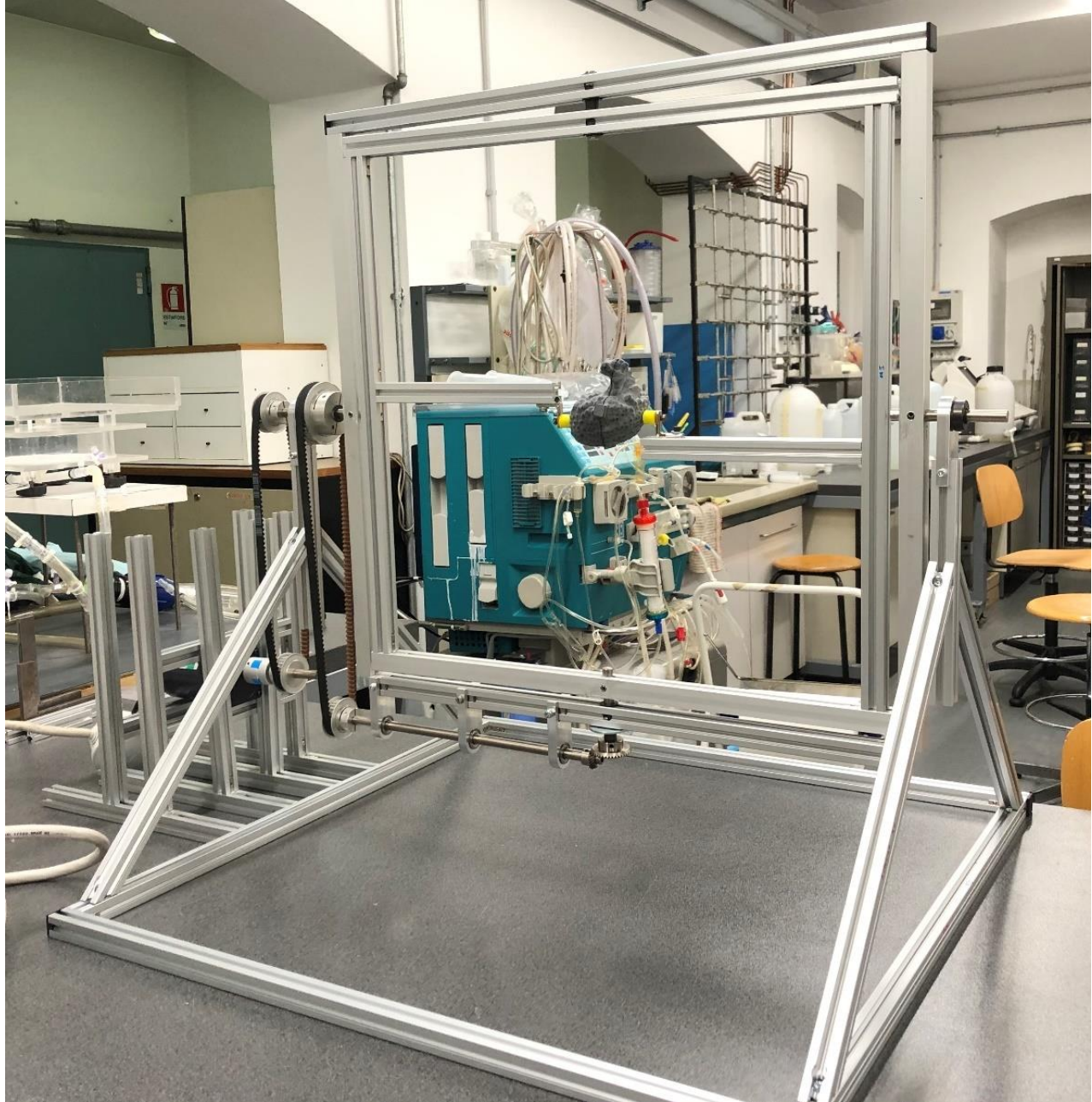
Figure 27: Final Rotocaster Design

To choose the motor, the maximum torque required must be calculated. To do that, the weights of all the components was found, and the total moment of inertia of the system was calculated.

In addition, the range of rotational speeds ω was determined to be between 0 and 20 rpm. Finally, with a safety factor of 2, the torque was calculated using the following equation:

$$\tau = I\alpha \,.\, Safety\ Factor = 2.04\ Nm \quad with \begin{cases} I: moment\ of\ inertia\ [kg.m^2] \\ \alpha: angular\ acceleration\ [\dfrac{rad}{s^2}] \end{cases}$$

Therefore, the maximum power needed is:

$$P = \tau\omega = 4.27\ W$$

According to these values, the motor was chosen.

IV.   Results

Several tests were done, varying one variable at a time, and keeping the others constant. To perform each experiment, we followed the same steps shown in the figure below.

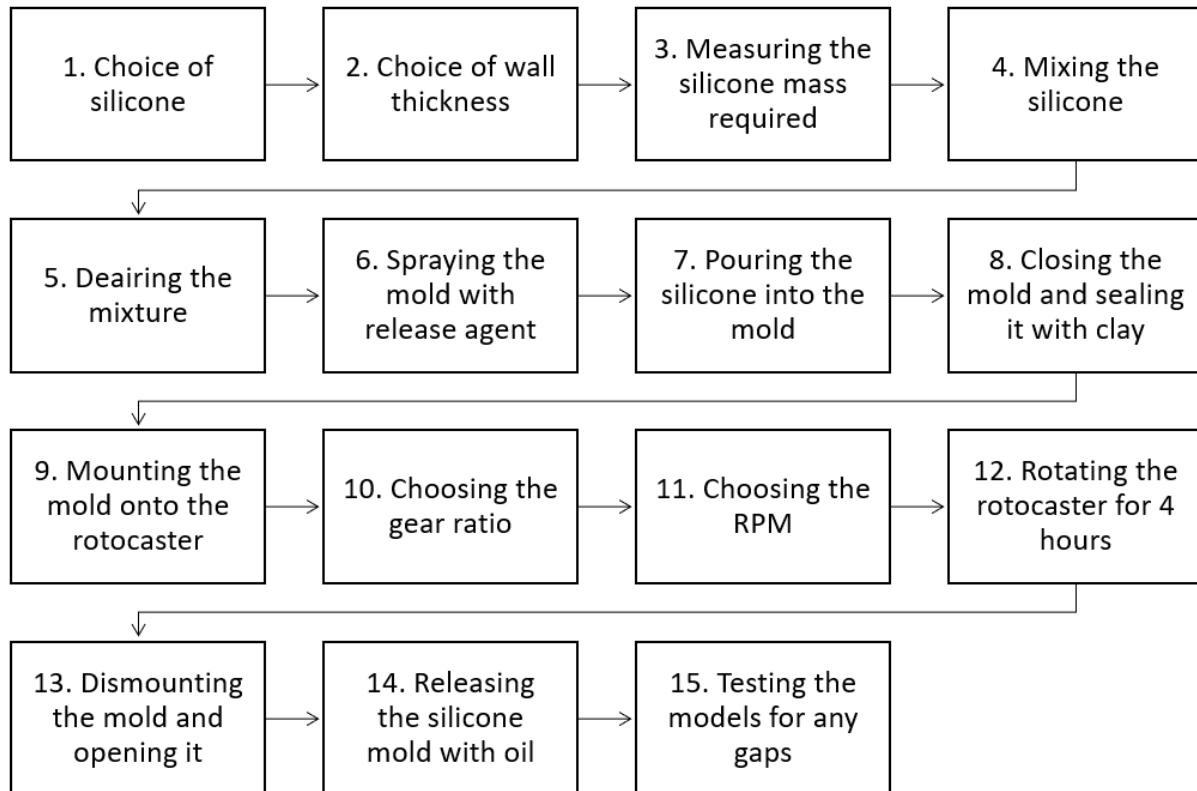| 1. Choice of silicone	2. Choice of wall thickness	3. Measuring the silicone mass required	4. Mixing the silicone
5. Deairing the mixture	6. Spraying the mold with release agent	7. Pouring the silicone into the mold	8. Closing the mold and sealing it with clay
9. Mounting the mold onto the rotocaster	10. Choosing the gear ratio	11. Choosing the RPM	12. Rotating the rotocaster for 4 hours
13. Dismounting the mold and opening it	14. Releasing the silicone mold with oil	15. Testing the models for any gaps	

Figure 28: Experimentation Process

i)   Test I

The first test was done using Dragon Skin 20 silicone and without the use of the rotational caster. To find the mass required for each desired wall thickness, we proceed by finding the volume of the mold, and then finding the volume of the offset of the mold by the desired thickness. Then, we subtract the two volumes to get the required volume.

The volume of the model was found on Meshmixer as V = 103161 mm^3 = 103.161 ml.

For a mold of wall thickness 2mm, we offset the model by 2mm, and the volume of the material required becomes:

$$V_{2mm} = 103.161 - 69.9224 = 33.2386 \; ml$$

The silicone contains two containers which need to be mixed in a 1:1 ratio. Since not provided, the density of both components was calculated by measuring the volume of the container and dividing the indicated mass by it:

$$\rho = \frac{0.45}{\pi(3.5^2)(12)(10^{-6})} = 974.42 \; kg/m^3$$

For a 2mm layer, the mass required is:

$$m = \rho V = 974.42 x 33.2386 x 10^{-3} = 32.39 \; g$$

Release agent (Ease Release 205) was sprayed on the inside of the mold and left for 10 minutes to dry. In the meantime, 17 grams of both components was measured to leave less than 2g of the mixture for observation. They were mixed for 2-3 minutes and placed in vacuum to degas for also 2-3 minutes. Next, the mixture was removed and poured into the left ventricle model which was manually and slowly rotated for more than an hour. Duct tape was placed at the edges to prevent silicone seeking. The model was rotated faster at first to prevent dripping, after which the speed was decreased with time. The silicone was left 4 hours to cure. The model was tested for any leakage, but none was detected; however, silicone was not able to reach the top area of the ventricle near the aortic valve.

The results of this test can be seen in the figures below.
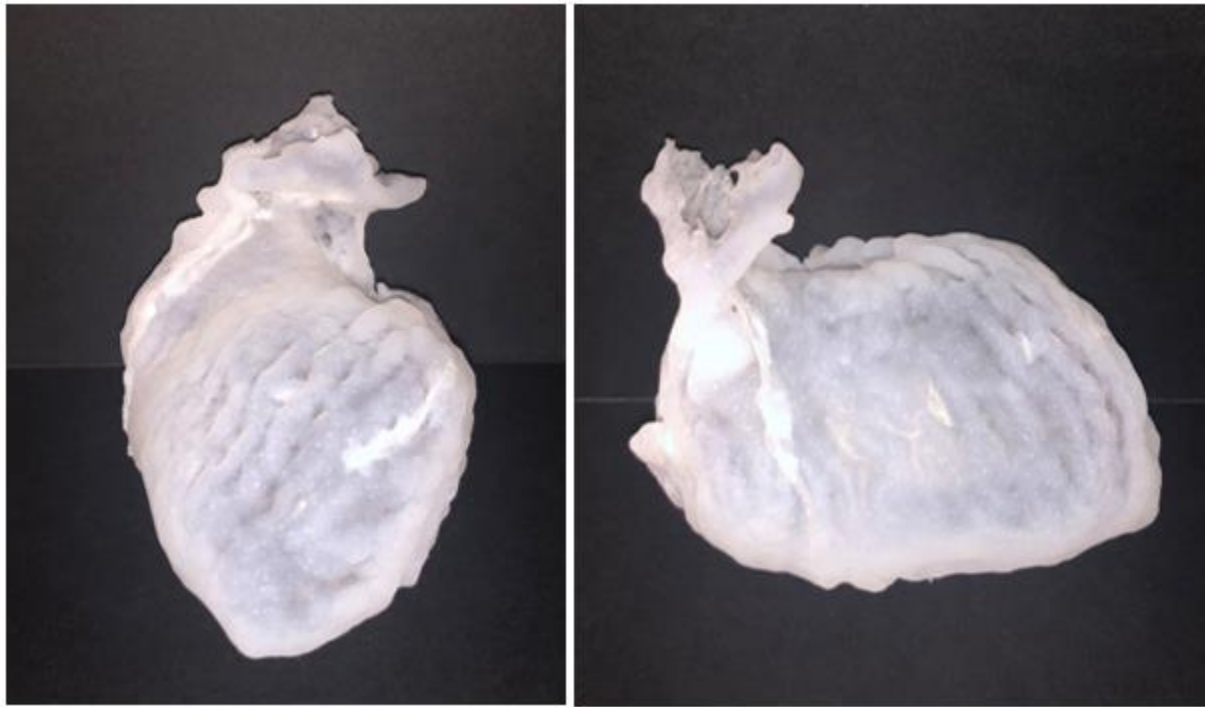
Figure 29: Results of Test I

ii)   Test II

In the second test, the rotocaster was used to test Dragon Skin 20 silicone again, using a 1:1 gear ratio. The wall thickness was kept at 2mm, such that if more thickness is required, an extra layer can be brushed on the outside.

After repeating the same steps as in test 1, some modeling clay was placed on the edges to prevent silicone from leaking to the outside after putting both halves together. The model was then mounted onto the rotocaster.

The model was rotated at 12 rpm for the first 30 minutes to prevent dripping, and then at 10 rpm for the next 3.5 hours while the silicone was left to cure.

The final model had several tears since the silicone was strongly stuck to the mold, which meant that we needed a stronger release agent. Also, the silicone accumulated at the restricted area on

the top part of the left ventricle and didn't reach the narrow part that connects the left ventricle to the aorta. Thus, in the next test we had to observe the effects of decreasing the rotational speed.
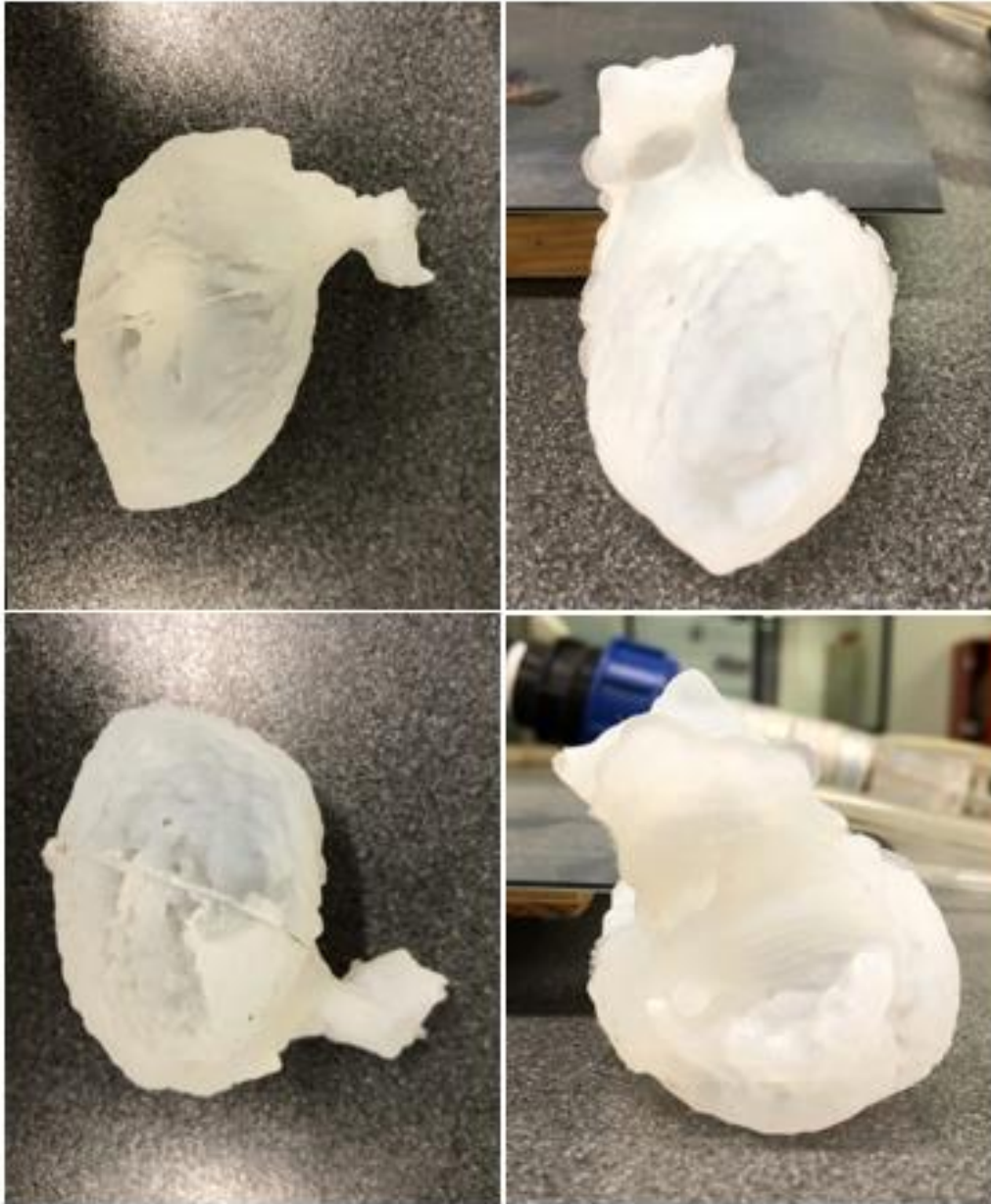

Figure 30: Results of Test II

iii)   Test III

In the third test, a different release agent was used (Ease Release 200), and the speed of rotation was varied. The model was rotated at 10 rpm for the first 30 minutes to prevent dripping, and then at around 8 rpm for the next 3.5 hours while the silicone was left to cure. Soap water was used to facilitate removing the mold.

The new release agent made it easier to remove the silicone mold and is recommended to be used in the other experiments. There was much less tearing in this mold compared to the previous one.

Because this silicone is relatively thick, reducing the RPM resulted in a better spreading in the silicone which can be seen in the reduced accumulation at the restricted area.
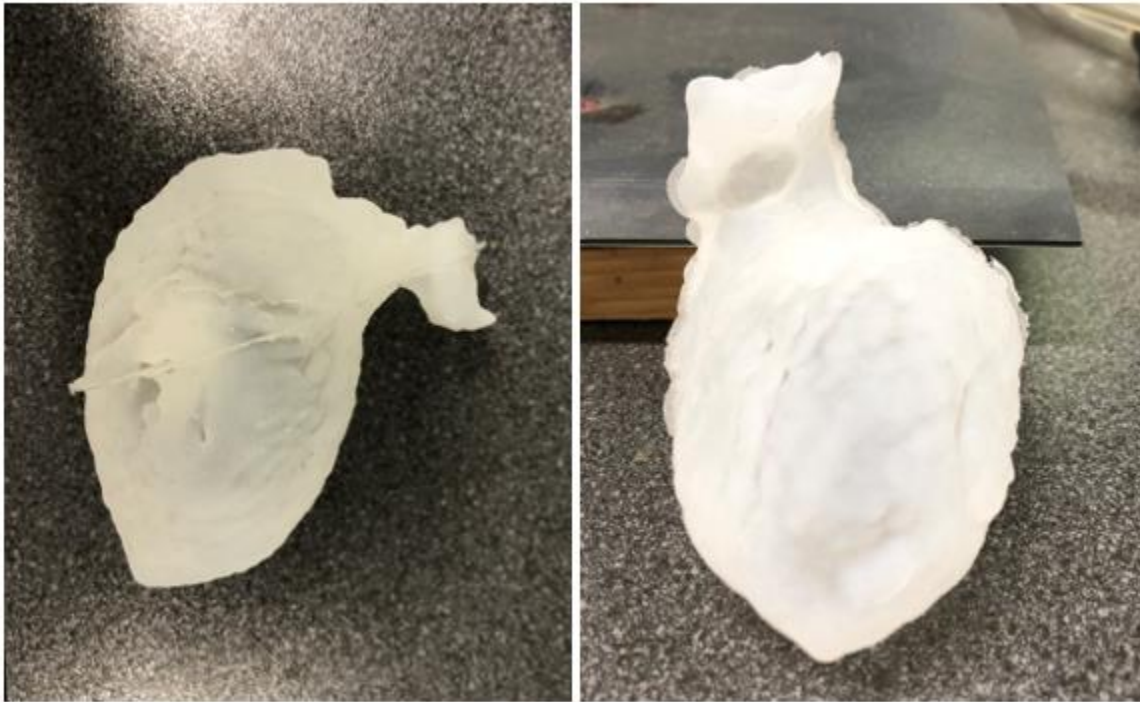
Figure 31: Results of Test III

iv)   Test IV

In this test, Dragon Skin 10 was used and the rotocaster was operated with a 1:1 gear ratio. We considered a wall thickness of 1mm, allowing us to brush silicone on the outer layer if required. Release agent (Ease Release 200) was sprayed on the mold and the test was repeated. Since

Dragon Skin 10 is thinner than Dragon Skin 20, it should not be rotated slowly to prevent dripping; thus, it was rotated at 8 rpm the whole time.

This model was the easiest to remove; however, the silicone was not spread uniformly, which means that a 1:1 gear ratio is not good for a thinner silicone.

Figure 32: Results of Test IV

V. Discussion

As shown in the results, many factors affect the final model. Using a thicker silicone requires a lower rotational speed to allow the silicone enough time to spread evenly to all sides. Whereas, using a thinner silicone could cause dripping during rotation, and therefore requires a faster rotational speed. Both types of silicone can be used, given that they are each treated accordingly.

Another factor is the wall thickness. After performing the tests, we have seen that a larger wall thickness prevented the silicone from seeping into narrow passages and caused it to accumulate in narrow areas. In addition, it didn't allow the silicone to recreate the details of the walls of the

model. However, the smaller wall thickness mimicked the details of the model much better. In addition, it was able to pass through any areas. It is recommended to always use a thinner wall which reproduces any required details, and brush silicone on the outside layer if needed to make it thicker.

The choice of gear ratio depends on the model at hand. For the left ventricle, a gear ratio of 1:1 allowed a very uniform silicone distribution. In general, the gear ratio is found by trial and error for each model. For more odd shapes, a gear ratio of 1:4 has been found to work well for example.

A release agent must always be used, especially for models with tight, narrow areas. Again, the choice of release agent depends on the material of the 3D printed molds and the model at hand and can be decided on via trial and error. Using oil or soap water to remove the model from the mold is recommended to prevent any tears while removing it.

Thus, we are able to make the following recommendations:

- A thick silicone must be rotated at a low speed at a 1:1 gear ratio.
- A thin silicone must be rotated at a slightly higher speed
- It is recommended to use a small wall thickness for two reasons: reducing accumulations in narrow passages and having a better reproduction of the inner wall.
- Using a release agent is necessary to be able to remove the silicone model without any tears.

After observing all the problems that could arise from this process, some future developments can be made. Specifically, to eliminate the problem of tearing while removing the silicone from the mold and to produce a more accurate surface.

The rotocaster produced a model which was highly accurate on the outside, but somewhat smooth on the inside. Having a wall thickness of 1 mm significantly reduced this problem but did not eliminate it.

To that aim, more left ventricle molds were created.

The first model is a core model to brush silicone on. This model is cut in half to make it possible to remove the silicone, and the two halves can then be joined with adhesive. There is no need for the rotocaster in this method. The challenges associated to this method is that it is difficult to control the wall thickness of the models, and we need to manually join the two halves which could lead to inaccuracies.
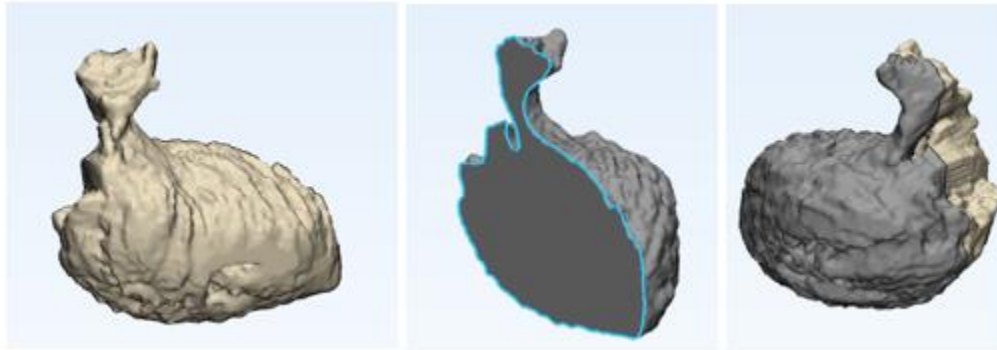
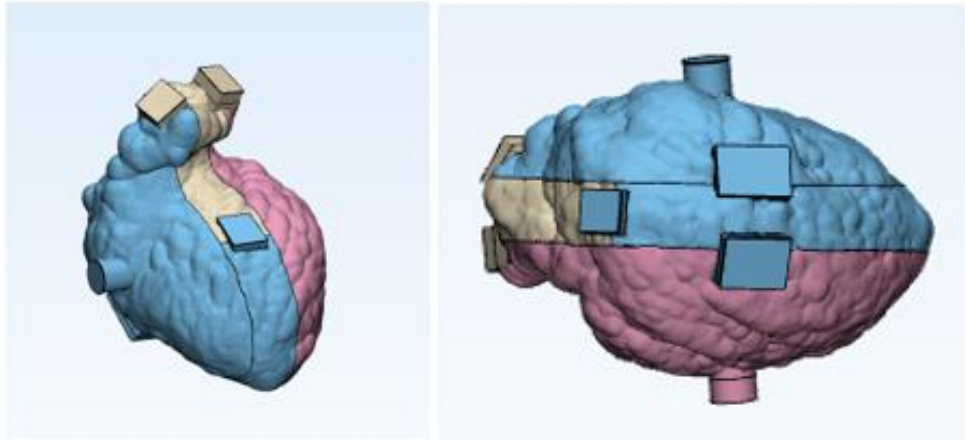*Figure 33: Brush-On Left Ventricle Mold*

The second model allows us to create an extremely precise inner surface. It results in a 3mm wall thickness and also doesn't require the use of the rotocaster. Silicone can be put into one half and the other half can be pressed onto it. The disadvantage is that the two halves have to be joined with an adhesive.
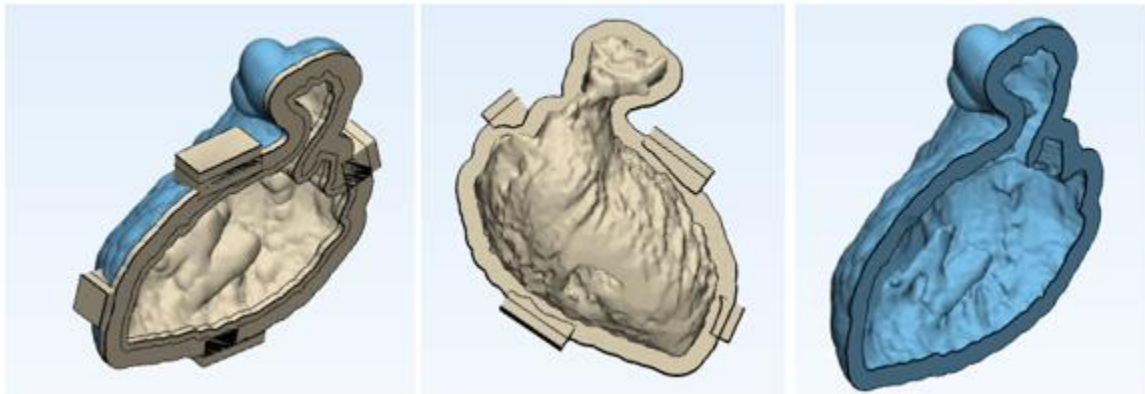
Figure 34: Press-On Left Ventricle Molds

The third model was meant to make the removal of the silicone easier. Again, it can be kept at a 1mm wall thickness, giving a good accuracy of the inner wall. It is composed of four parts and requires the use of a rotocaster.

Figure 35: Four-Part Left Ventricle Mold

Similar models were created for the aorta. A core model to brush silicone on was divided into four parts which must be joined with an adhesive (model 1). The second model requires the use of the rotocaster. The aorta was divided into four parts that can be attached and detached. Two holders were added for the inserts (model 2).
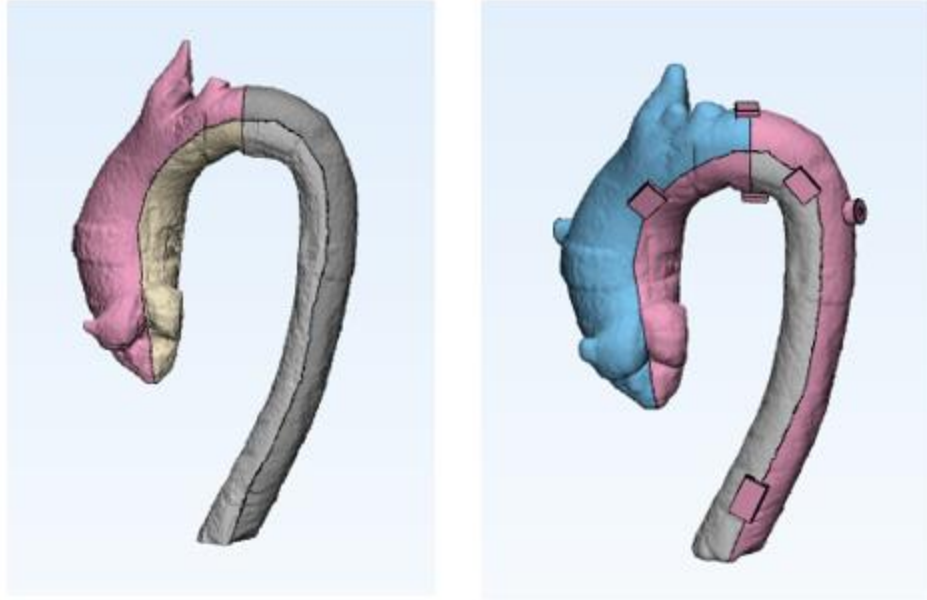
Figure 36: Aorta Molds (Model 1 on the Left, Model 2 on the Right)

VI.   Conclusion and Future Developments

The fabrication of 3D models which mimic the human organs is a more than feasible topic. The created models are accurate enough for experimentation and developments in medicine. Whether it be with or without the help of rotational casting, 3D printing alone is not sufficient. Rotational casting is one of the methods used to take a 3D printed organ one step further. It can produce accurate models with a fast pace and will prove to be highly reliable.

This study has shown that with the correct combination of parameters, it is possible to create any organ with its desired strength, thickness, and flexibility. Rotational casting provides us with the ability to utilize a very wide range of materials and shapes with very minimal waste, something that many other methods lack.

In conclusion, with the help of image processing techniques, 3D printing and casting methods, experimentation for medical purposes will be more feasible and reliable. Rotational casting is a highly recommended casting technique that must be looked into more.

Appendix A

List of Components

Item	Material	Dimensions	Quantity
Aluminum Frames (20x20)	Aluminum	L=650mm	2
	Aluminum	L=600mm	2
	Aluminum	L=560mm	2
	Aluminum	L=540mm	2
	Aluminum	L=500mm	2
	Aluminum	L=300mm	4
	Aluminum	L=200mm	8
Brackets for Reinforcement	Aluminum	L=300mm	4
Ball Bearings	Steel	D_{in}=10mm, D_{out}=19mm, W=5mm	10
Belts	Rubber	L=710mm	1
	Rubber	L=830mm	1
	Rubber	L=870mm	1
Spiral Bevel Gears	Steel	N=20, D=10mm	1
	Steel	N=30, D=10mm	2
	Steel	N=40, D=10mm	1
Blind Brackets	SCS13	Slot Width 6mm	16
Oil Free Bushings	iglide G300	Din=10mm, Dout=12mm, L=11mm	10
Clamp Pulleys	Aluminum	D_{bore}=10mm, N=24	3
	Aluminum	D_{bore}=10mm, N=40	2
Coupling	Aluminum	D_{bore}=10mm (Clamping Type with Keyway)	1
	Aluminum	D1=10mm, D2=8mm	1
End Caps	Resin	20x20	6
Hollow Rotary Shaft	S45C	D=10mm, L=335mm	1
Rotary Shafts	S45C	D=10mm, L=78.8mm	1
	S45C	D=10mm, L=91mm	1
	S45C	D=10mm, L=130mm	1
	S45C	D=10mm, L=80mm	1
Shaft with Retaining Rings	S45C	D=10mm, L=58mm	1
Springs		D=12mm, L=10mm	2
		D=12mm, L=15mm	2

Spring Pins	Stainless Steel	D=6mm, L=22mm	10
Sleeve Bearing	iglide G	D=10mm, L=8mm	3
	iglide G	D=10mm, L=9mm	3
Insertion Nuts	Stainless Steel	M4 Thread	18
Shaft Collar	S45C	D=10mm	2
Bearing Holders	Aluminum	Drawing Available	5
Hollow Rotary Shaft	S45C	L=320mm, D=10mm	1
Oil Free Bushings	iglide G300	D=6mm	8
Belt	Rubber	L=787.4mm	2
Aluminum Frames	Aluminum	L=340mm	2
	Aluminum	L=100mm	2
Bevel Gears	Steel	D=6mm, N=20	1
	Steel	D=10mm, N=20	1
Pulleys	Aluminum	D=10mm, N=30	1
	Aluminum	D=10mm, N=22	2
Pulleys			2
Tabbed Reversal Brackets	ADC12	M5	12

Table 5: List of Components for the Rotational Caster
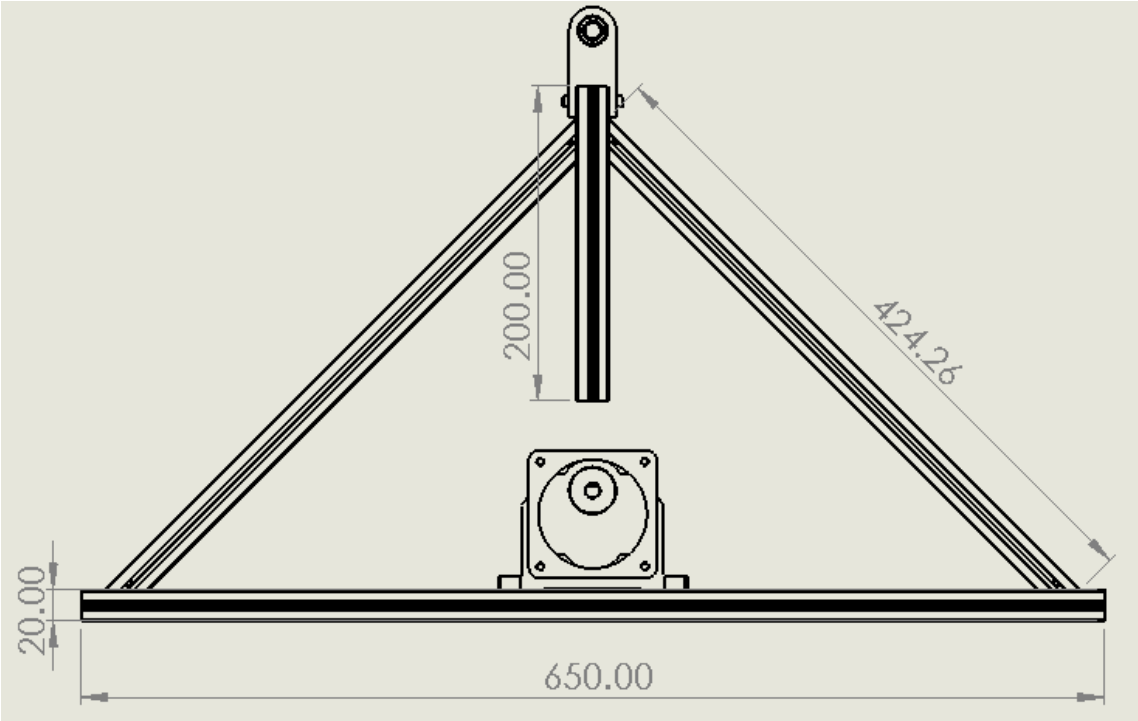
Technical Drawings

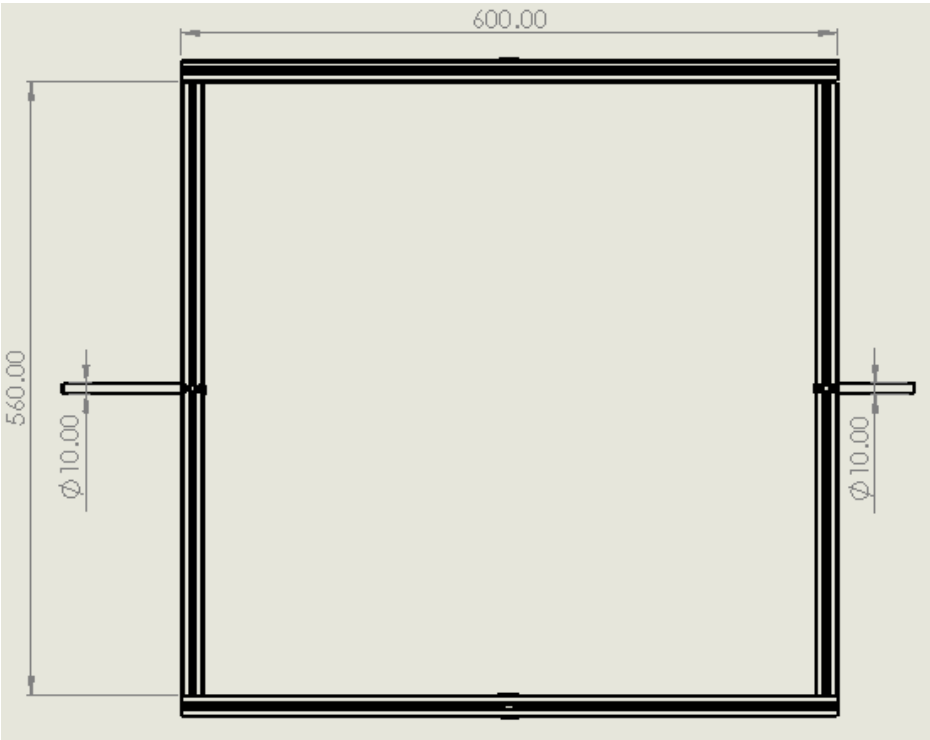*Figure 37: Technical Drawing of the Support Frame*

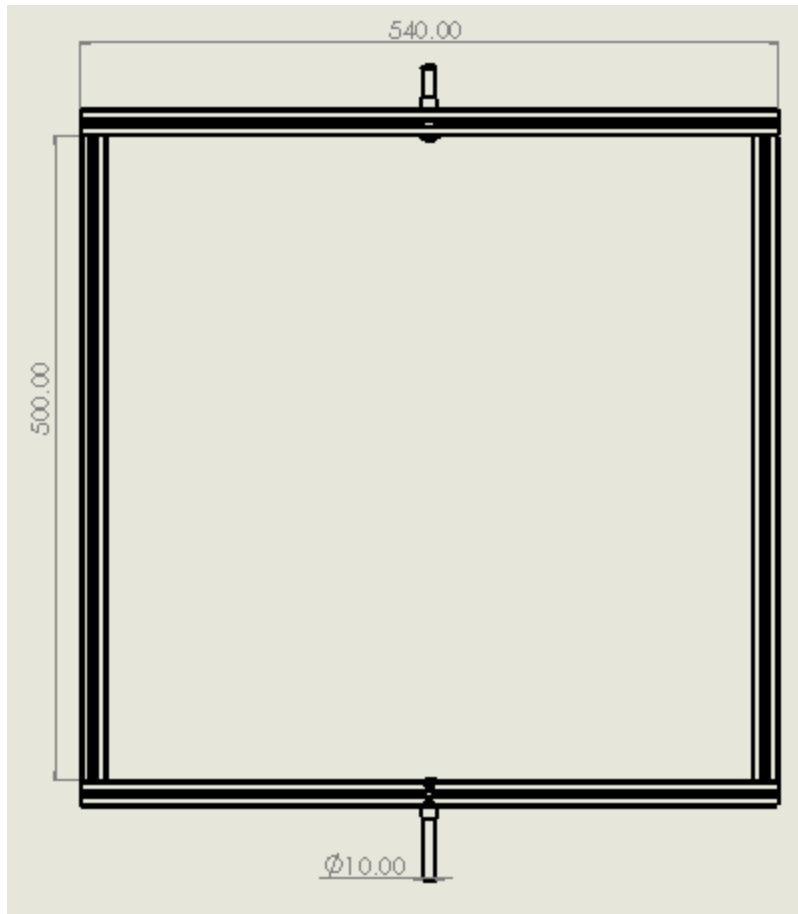
Figure 38: Technical Drawing of the Outer Frame
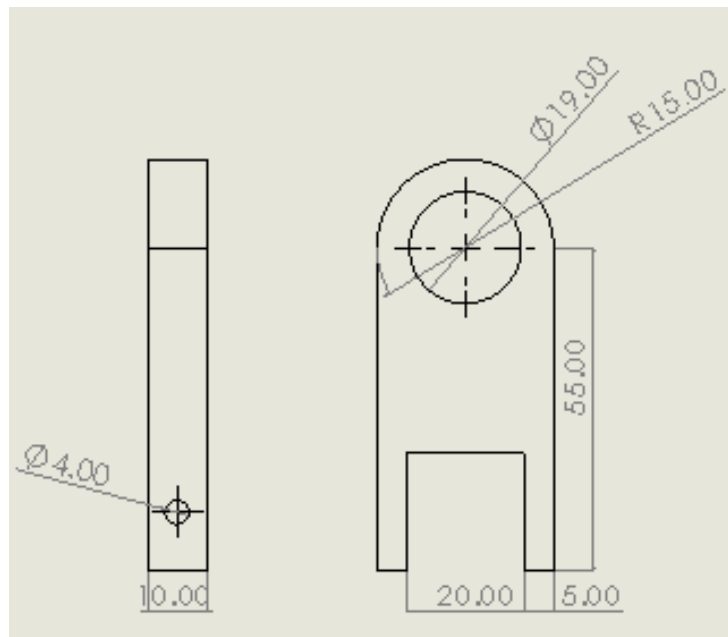
Figure 39: Technical Drawing of the Inner Frame

Figure 40: Technical Drawing of the Bearing Holder

Bibliography

[1] Martens, S., Sodemann, C., Doss, M., Neumann, K., Wimmer-Greinecker, G., Deschka, H., Dietrich, M., & Moritz, A. (2006). Carbon Dioxide Field Flooding Reduces Neurologic Impairment After Open Heart Surgery. Innovations: Technology and Techniques in Cardiothoracic and Vascular Surgery, 1(4), 216. https://doi.org/10.1097/01243895-200600140-00120

[2] Nyman, J., Svenarud, P., & van der Linden, J. (2019). Carbon dioxide de-airing in minimal invasive cardiac surgery, a new effective device. Journal of Cardiothoracic Surgery, 14(1), 1–8. https://doi.org/10.1186/s13019-018-0824-4

[3] Kimberly L. Skidmore, Clinton Jones, Charl DeWet (2006). Flooding the Surgical Field With Carbon Dioxide During Open Heart Surgery Improves Segmental Wall Motion. https://www.ncbi.nlm.nih.gov/pmc/articles/PMC4680747/

[4] Webb, W. R., Harrison, L. H., Helmcke, F. R., Camino-Lopez, A., Munfakh, N. A., Heck, H. A., & Moulder, P. V. (1997). Carbon Dioxide Field Flooding Minimizes Residual Intracardiac Air After Open Heart Operations. The Annals of Thoracic Surgery, 64(5), 1489–1491. https://doi.org/10.1016/s0003-4975(97)00945-4

[5] Ng, W. S., & Rosen, M. (1968). Carbon dioxide in the prevention of air embolism during open-heart surgery. Thorax, 23(2), 194–196. https://doi.org/10.1136/thx.23.2.194

[6] Rengier, F., Mehndiratta, A., von Tengg-Kobligk, H., Zechmann, C. M., Unterhinninghofen, R., Kauczor, H. U., & Giesel, F. L. (2010). 3D printing based on imaging data: review of medical

applications. International Journal of Computer Assisted Radiology and Surgery, 5(4), 335–341. https://doi.org/10.1007/s11548-010-0476-x

[7] Otton, J. M., Birbara, N. S., Hussain, T., Greil, G., Foley, T. A., & Pather, N. (2017). 3D printing from cardiovascular CT: a practical guide and review. Cardiovascular Diagnosis and Therapy, 7(5), 507–526. https://doi.org/10.21037/cdt.2017.01.12

[8] Friedman, T., Michalski, M., Goodman, T. R., & Brown, J. E. (2015). 3D printing from diagnostic images: a radiologist's primer with an emphasis on musculoskeletal imaging—putting the 3D printing of pathology into the hands of every physician. Skeletal Radiology, 45(3), 307–321. https://doi.org/10.1007/s00256-015-2282-6

[9] Lee, S. M., Lee, J. G., Lee, G., Choe, J., Do, K. H., Kim, N., & Seo, J. B. (2019). CT Image Conversion among Different Reconstruction Kernels without a Sinogram by Using a Convolutional Neural Network. Korean Journal of Radiology, 20(2), 295. https://doi.org/10.3348/kjr.2018.0249

[10] Aggarwal, P., Vig, R., Bhadoria, S., & C.G.Dethe, A. (2011). Role of Segmentation in Medical Imaging: A Comparative Study. International Journal of Computer Applications, 29(1), 54–61. https://doi.org/10.5120/3525-4803

[11] Schubert, C., van Langeveld, M. C., & Donoso, L. A. (2013). Innovations in 3D printing: a 3D overview from optics to organs. British Journal of Ophthalmology, 98(2), 159–161. https://doi.org/10.1136/bjophthalmol-2013-304446

[12] Gordon M. Paul, Amin Rezaienia, Pihau Wen, Sridhar Condoor, Nadeem Parkar, Wilson King, Theodosios Korakianitis (2018). Medical Applications for 3D Printing: Recent Developments. Missouri Medicine, 115(1), 75-81. https://www.ncbi.nlm.nih.gov/pmc/articles/PMC6139809/

[13] George, E., Liacouras, P., Rybicki, F. J., & Mitsouras, D. (2017). Measuring and Establishing the Accuracy and Reproducibility of 3D Printed Medical Models. RadioGraphics, 37(5), 1424–1450. https://doi.org/10.1148/rg.2017160165

[14] Melocchi, A., Parietti, F., Loreti, G., Maroni, A., Gazzaniga, A., & Zema, L. (2015). 3D printing by fused deposition modeling (FDM) of a swellable/erodible capsular device for oral pulsatile release of drugs. Journal of Drug Delivery Science and Technology, 30, 360–367. https://doi.org/10.1016/j.jddst.2015.07.016

[15] Palermo, E. (2013, September 20). Fused Deposition Modeling: Most Common 3D Printing Method. Livescience.Com. https://www.livescience.com/39810-fused-deposition-modeling.html

[16] Xu, X., Robles-Martinez, P., Madla, C. M., Joubert, F., Goyanes, A., Basit, A. W., & Gaisford, S. (2020). Stereolithography (SLA) 3D printing of an antihypertensive polyprintlet: Case study of an unexpected photopolymer-drug reaction. Additive Manufacturing, 33, 101071. https://doi.org/10.1016/j.addma.2020.101071

[17] The Ultimate Guide to Stereolithography (SLA) 3D Printing. (2020). Formlabs. https://formlabs.com/asia/blog/ultimate-guide-to-stereolithography-sla-3d-printing/

[18] Fina, F., Goyanes, A., Gaisford, S., & Basit, A. W. (2017). Selective laser sintering (SLS) 3D printing of medicines. International Journal of Pharmaceutics, 529(1–2), 285–293. https://doi.org/10.1016/j.ijpharm.2017.06.082

[19] Guide to Selective Laser Sintering (SLS) 3D Printing. (2020). Formlabs. https://formlabs.com/asia/blog/what-is-selective-laser-sintering/

[20] Galati, M., Calignano, F., Defanti, S., & Denti, L. (2020). Disclosing the build-up mechanisms of multi jet fusion: Experimental insight into the characteristics of starting materials and finished parts. Journal of Manufacturing Processes, 57, 244–253. https://doi.org/10.1016/j.jmapro.2020.06.029

[21] Gaget, L. (2019, July 16). 3D printing and traditional manufacturing processes. 3D Printing Blog: Tutorials, News, Trends and Resources | Sculpteo. https://www.sculpteo.com/blog/2019/07/16/comparison-between-3d-printing-and-traditional-manufacturing-processes-for-plastics-3

[22] Ogila, K. O., Shao, M., Yang, W., & Tan, J. (2017). Rotational molding: A review of the models and materials. Express Polymer Letters, 11(10), 778–798. https://doi.org/10.3144/expresspolymlett.2017.75

[23] How to Design and Install Bevel Gears for Optimum Performance - Lessons Learned : Gear Technology June/July 2013. (2013). Gear Technology. https://www.geartechnology.com/articles/0613/How_to_Design_and_Install_Bevel_Gears_for_Optimum_Performance_-_Lessons_Learned/

[24] Cohrs, N. H., Petrou, A., Loepfe, M., Yliruka, M., Schumacher, C. M., Kohll, A. X., Starck, C. T., Schmid Daners, M., Meboldt, M., Falk, V., & Stark, W. J. (2017). A Soft Total Artificial Heart-First Concept Evaluation on a Hybrid Mock Circulation. Artificial Organs, 41(10), 948–958. https://doi.org/10.1111/aor.12956

[25] Smooth-On, Inc. (2010). Mold Making & Casting Materials | Rubbers, Plastics, Foams & More! https://smooth-on.com

[26] Dé Europese leverancier voor vormmaterialen en -systemen. (2020, December 3). Schouten Group. https://schoutengroup.com